Appendix 1 to Combined Description of Preparation, Defence and Keeping of Final Projects

KAUNAS UNIVERSITY OF TECHNOLOGY

MECHANICAL ENGINEERING AND DESIGN FACULTY

KISHAN NARASIMHAMURTHY

NUMERICAL ANALYSIS OF METAL FORMING PROCESS

Final project for Bachelor/Master degree

Supervisor
Assoc. Prof. Dr. Paulius Griskevicius

KAUNAS, 2016

KAUNAS UNIVERSITY OF TECHNOLOGY
MECHANICAL ENGINEERING AND DESIGN FACULTY

NUMERICAL ANALYSIS OF METAL FORMING PROCESS

Final project for Bachelor/Master degree
MASTERS IN MECHANICAL ENGINEERING (code 621H30001)

Supervisor
(signature) Assoc. Prof. Dr. Paulius Griskevicius
(date)

Reviewer
(signature) Assoc. Prof. Dr. Marius Rimasauskas
(date)

Project made by
(signature) KISHAN NARASIMHAMURTHY
(date)

KAUNAS, 2016

Appendix 1 to Combined Description of Preparation, Defence and Keeping of Final Projects

KAUNAS UNIVERSITY OF TECHNOLOGY

MECHANICAL ENGINEERING AND DESIGN FACULTY

(Faculty)

KISHAN NARASIMHAMURTHY

(Student's name, surname)

MASTERS IN MECHANICAL ENGINEERING ME M-3/2

(Title and code of study programme)

NUMERICAL ANALYSIS OF METAL FORMING PROCESS

DECLARATION OF ACADEMIC HONESTY

___ _____ 20 16

Kaunas

I confirm that a final project by me, KISHAN NARASIMHAMURTHY, on the subject "NUMERICAL ANALYSIS OF METAL FORMING PROCESS." is written completely by myself; all provided data and research results are correct and obtained honestly. None of the parts of this thesis have been plagiarized from any printed or Internet sources, all direct and indirect quotations from other resources are indicated in literature references. No monetary amounts not provided for by law have been paid to anyone for this thesis.

I understand that in case of a resurfaced fact of dishonesty penalties will be applied to me according to the procedure effective at Kaunas University of Technology.

(name and surname filled in by hand) *(signature)*

NARASIMHAMURTHY. Metalų formavimo procesų skaitinė analizė. Mechanikos inžinerijos Magistro baigiamasis PROJEKTAS/ supervisor Assoc. Prof. Dr. Paulius Griskevicius; Kaunas University of Technology, Mechanikos inžinerijos ir dizaino fakultetas, Mechanikos inžinerijos katedra.

Kaunas, 2016. 58 p.

SUMMARY

Santrauka

Darbe palyginamoji analizė skirtingų medžiagų modelių tinkamumo metalų formavimo procesų simuliacijai. Pasirinkta medžiaga – vidutinio stiprumo plastiškas plienas, naudojamas automobilio kėbulų gamybai. Eksperimentiškai nustatytos mechaninės medžiagos savybės aproksimuotos trim skirtingais medžiagos modeliais įdiegtais baigtinių elementų programoje LS-Dyna. Simuliuojant metalų formavimo procesus svarbus yra formavimo ribinės diagrams (Forming limit diagram FLD) kriterijus, kuris įprastai turėtų būti gaunamas eksperimentiškai naudojant sudėtingos formos bandinius ir bekontaktę deformacijų matavimo sistemą. Šiame darbe natūriniai FLD kreivės nustatymo eksperimentai pakeisti skaitiniais eksperimentais, t.y. programoje LS-Dyna simuliuoti FLD kreivės nustatymo eksperimentai, kurie palyginti su empirinių formulių rezultatais. Gauti sutapimai parodė, kad turint tikslią medžiagos tempimo diagramą, galima skaitiniu eksperimentu gauti FLD kreivę, kuri yra naudojama metalų formavimo procesuose įvertinti deformuojamos medžiagos būvį. Darbe taip pat palyginti išduobimo eksperimentiniai rezultatai su skaitiniais, pritaikius FLD kreivės kriterijų įvertinti skirtingi medžiagos būviai ir vizualiai palyginti su natūrniu eksperimentus, bei įvertinta atskirų parametrų įtaka skaičiavimo rezultatams.

Raktiniai žodžiai: Ribinė formavimo diagrama (FLD), išduobimo bandymas, tempimo bandymas, baigtinių elementų analizė.

Summary

In this work are presented the comparison analysis of different material models suitability to simulate metal forming processes. Chosen material is the mid strength and plastic steel from automotive body. Experimentally defined mechanical properties of material were approximated using three different material models from Finite element program LS-Dyna. For simulation of metal forming processes important is Forming limit diagram FLD criteria, which usually is obtained from complex form geometry and using noncontact strain measurement system. In this work the physical determination of FLD curve is replaced by numerical experiments. The FLD curve is determined using the FE simulation in LS-Dyna and compared with FLD from empirical formulas. Good coincidence of results showed that having proper tension curve of material, it is possible to simulate the FLD curve. This curve is commonly used in the metal forming processes for the evaluation of state of deformed material. The comparison of physical cupping test and numerical simulation are presented also. Using FLD criteria the different states of the material are obtained and visually compared with the experiments. Also the influence of separate parameters to the behavior of material during the metal forming process are evaluated.

Keywords: Forming limited diagram (FLD) curves, Cupping test, Tension test, finite element method.

Contents

Introduction

The metal forming process is the most common procedure which are used in most of the mechanical industries. Main mechanisms can cause the fracture of a ductile metal are necking, growth and joining of holes and shear fracture due to shear band localization. Necking is the main parameter in metal forming operation. The purpose of this study is to develop a phenomenological model for prediction of the entire forming limit diagram from simple tensile material properties. The forming limit curves calculated from the proposed phenomenological model matched sensibly well in the region of uniaxial tension to balance biaxial tension with the theoretical forming limit curves created. The formability limit of sheet metal is obtained by the initiation of the local neck that leads to fracture.

.

Aim

Comparing with the experimental results evaluate the existed approaches in FE code LS-Dyna and LS-PrePost for simulation of sheet metal forming processes.

Tasks:

1. Compare the FLD curves obtained using different approaches, theoretical-empirical formulas, LS-PrePost tool and FE simulation of natural experiments;
2. Evaluate the usage of Forming Limit Diagram (FLD) criteria implemented in LS-PrePost for prediction of material formability before building the real metal forming tools;
3. Evaluate the suitability of widely used material models to the simulation of metal forming process and influence of some parameters to the results;
4. Identify the influence of FE mesh size to the results of metal forming process simulation.

1. Metal forming processes and Forming limit diagram

1.1History of metal forming

Steel is one of the world's most essential materials. It is fundamental to every aspect of our lives, from infrastructure and transport to the humble tin-plated steel can that preserves food. With steel, we can create huge buildings or tiny parts for precision instruments. It is strong, versatile and infinitely recyclable. The rise of steel began with the 19th century Industrial Revolution in Europe and North America. Yet steelmaking isn't new. Master craftsmen in ancient China and India were skilled in its production. However, it is only in the past 200 years that science has revealed the secrets of this remarkable material. Today, steelmakers know how to combine the exact mix of iron, a small percentage of carbon and other trace elements to produce hundreds of types of steel. These are then rolled, annealed and coated to deliver tailor-made properties for innumerable applications. Steelmakers continue to reduce the energy required to make steel. Modern high-strength steels provide more strength with less weight, helping reduce the emissions of carbon dioxide of end products such as cars. And because steel can be so easily recycled, supplies will remain abundant for generations to come. [1]

Since the nineteenth century, the response of a metal sheet subjected to sheet working conditions has been afforded much attention, especially as regards hardening, anisotropic and formability behavior, giving rise to a large amount of literature. A wide range of tests is actually available to reproduce the material behavior as well as numerous models to describe the different phenomena that characterize the metal response. In sheet metals, the response to plastic deformation shows itself through different processes, such as hardening, anisotropy, failure, and fracture.[12] Most of these processes occur simultaneously with important interactions and may deeply affect the behavior of the sheet metal due to the significant changes they cause in its physical and mechanical features and properties, such as surface appearance and roughness, yield-point elongation, resistance to plastic deformation, hardness and strength, residual stresses and geometric distortion, spring back, and formability. In the scientific and technical literature, testing and modeling of material behavior in sheet metal forming are distributed with separately from bulk metalworking. Even if the sheet metal products like deep drawing, rolling will be the deformation mostly occurs by the tensile force in the plane rather than by compression and mechanics of sheet forming basically consists of stretching and bending. Sheet metal forming includes a wide range

of enlargements that manufacture parts for the enormous quantity of purposes, both seen and unseen. Sheet metal refers to the metal that has a high surface area to volume ratio. Sheet metal work stock, used for sheet metal processes, is usually formed by rolling and arises in coils.

Sheet metal will be used for the different purposes and this is having very large applications in the market. They are used as the different structural parts like boilers, turbines, and ships. Sheet metal is used in the manufacture of trains, automobiles, aircraft, farm equipment, furniture, computers, machine components and beverage cans and so on. Few sheet metal manufacturing methods may be applicable to plate metal as well, even though the workpiece is referenced only as sheet metal. Sheet metal manufacturing is mostly performed on a press and parts are formed between two dies. Punch is the top die. Sometimes sheet metal parts are referenced to as stampings. Parts are usually cost effective and easy for mass production. Sheet metals can be work on the cold or hot formed on the hot working parts. Generally, in sheet metal works the change in the thickness will be very less or negligible. In some cases like deep drawing, there will be a very small changes in the thickness in the sheet metal and sometimes that change will be neglected. Sheet metal manufacturing produces parts that typically have high strength, good surface, and accurate tolerances.

While manufacturing the sheet metal products, mechanical behavior roles an important role. The metal forming basics section provides information on this topic. Mostly, metals will be having a more plastic deformation before necking. When necking of the metal occurs, diffuse necking is preferred over localized necking. Materials with high total deformation are more suitable for the sheet metal works. Some metals may have low carbon steels and aluminum-magnesium alloys may experience yield point elongation. This uneven yielding of the material may produce stretcher strains. Grains will affect the surface fish of the sheet metal surface. These lines are actually small depressions in the material. Grain size, structure and orientation are also important in a sheet metal work piece. In addition to the standard tests for materials, (such as tension tests), there are tests that are used specifically to determine the formability of sheet metal. One common test is the cupping test. A specimen is placed over the round die with the cavity. Then the steel ball from the top will be pushed to the specimen which is placed securely on the die. The ball is pushed until the specimen gets a fracture. The greater the distance the sheet deforms plastically, greater the sheet's formability.

Anisotropy is an important factor in sheet metal forming. Anisotropy is the directional variation of mechanical properties. In other words, the material which behaves differently to stress applied in the single direction than it would to the same stress applied in different directions. If the properties are same

in all the direction then it is isotropic. Cupping tests can be used to determine anisotropy. If the fracture occurring due to the applied force through the round ball is circular, then the sheet is isotropic. If a straight fracture occurs, this means that the sheet is anisotropic.

Many sheet metal operations will create a complex distribution of forces. Material elements experience different amounts, and proportions, of bi-axle stress and strain depending upon their location within the work. Sometimes a sheet metal is tested over a range of different bi-axle forces. A grid with inscribed circles is printed on the specimen. The grid and circles will deform with the metal. To determine, the metal's reaction for the different combinations of bi-axle strain tests will be conducted.

The different types of metal forming are as follows.

1.2Metal forming process

Rolling. Rolling is a metal forming process that deforms the work by the use of rolls. Rolling processes include flat rolling, shape rolling, ring rolling, thread rolling, gear rolling, and the production of seamless tube and pipe by rotary tube piercing or roll piercing.

Fig 1.1 schematic representation of rolling process[15]

Forging. Forging is characteristic in the use of dies to compress and shape a work piece. The die may be flat or may contain an impression of a certain geometry.

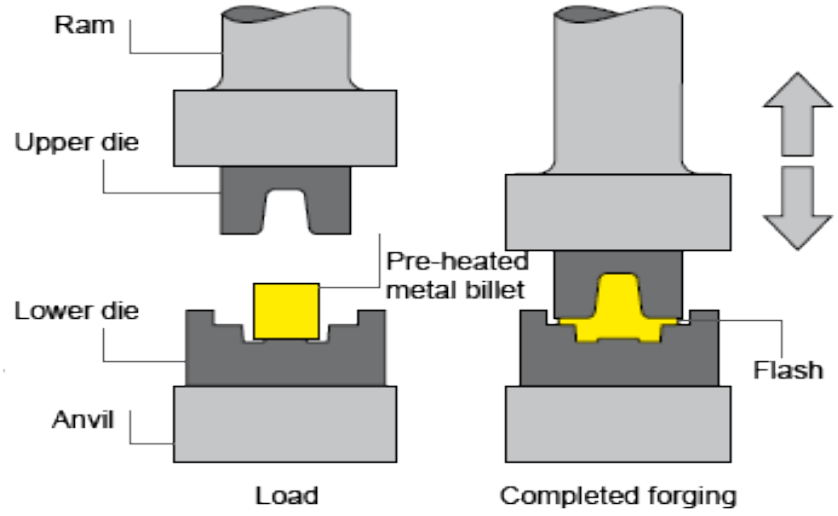

Fig 1.2 schematic representation of forging process [15]

Extrusion. Extrusion involves forming by forcing metal through a die opening, producing work of variable length and constant cross section.

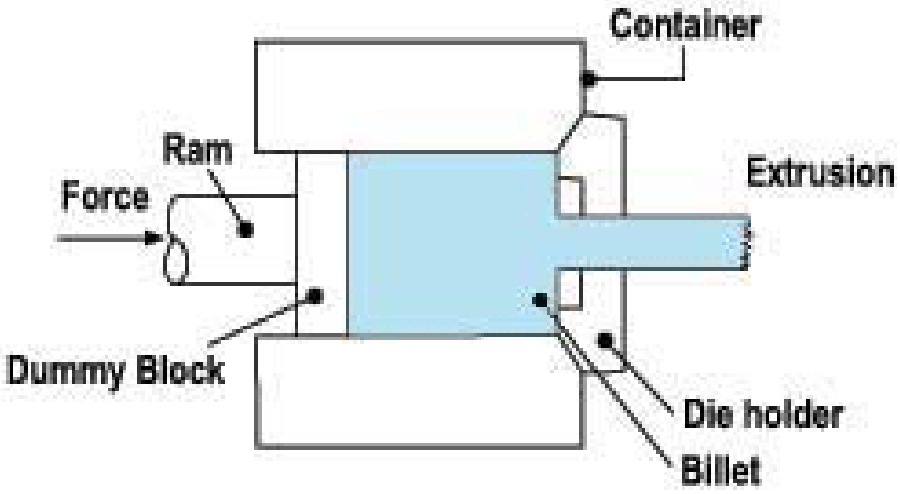

Fig 1.3 schematic representation of extrusion process[17]

Drawing. Drawing is similar to extrusion, in that a length of metal is made to flow through a die opening and forming is done over its cross section. The difference between drawing and extrusion is the application of force to the work piece. In extrusion the work is pushed through the die opening, in drawing the work is pulled through the die opening.

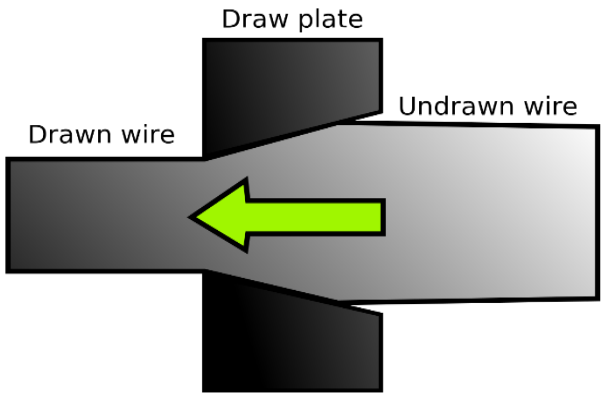

Fig 1.4 schematic representation of drawing process [17]

Shearing. Shearing is the cutting of the work piece, this would include punching holes. Technically shearing does not involve shaping by plastic deformation, but it is a critical process in sheet metal working operations and should be understood along with metal forming process.

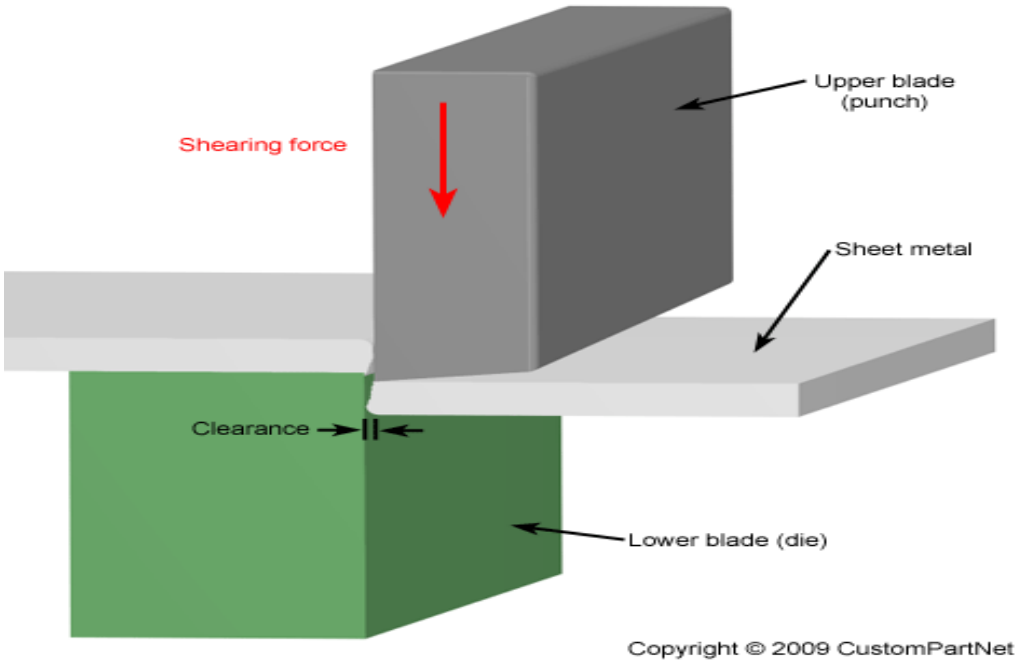

Fig 1.5 schematic representation of shearing process [18]

Deep Drawing. Deep drawing is a metal forming process in which a flat piece of plate or sheet is forced into a die cavity to take a shape, such as a cup.

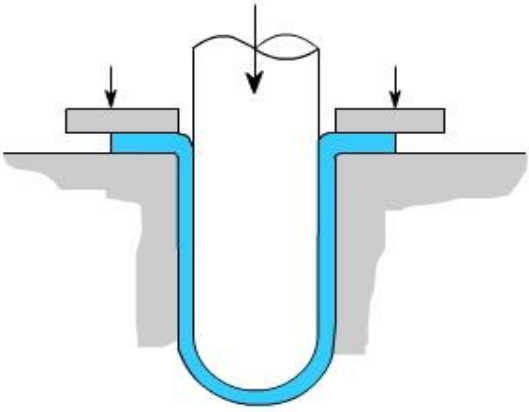

Fig 1.6 schematic representation of deep drawing process [18]

Bending. Bending involves the deformation of the work by way of bending about a certain axis.

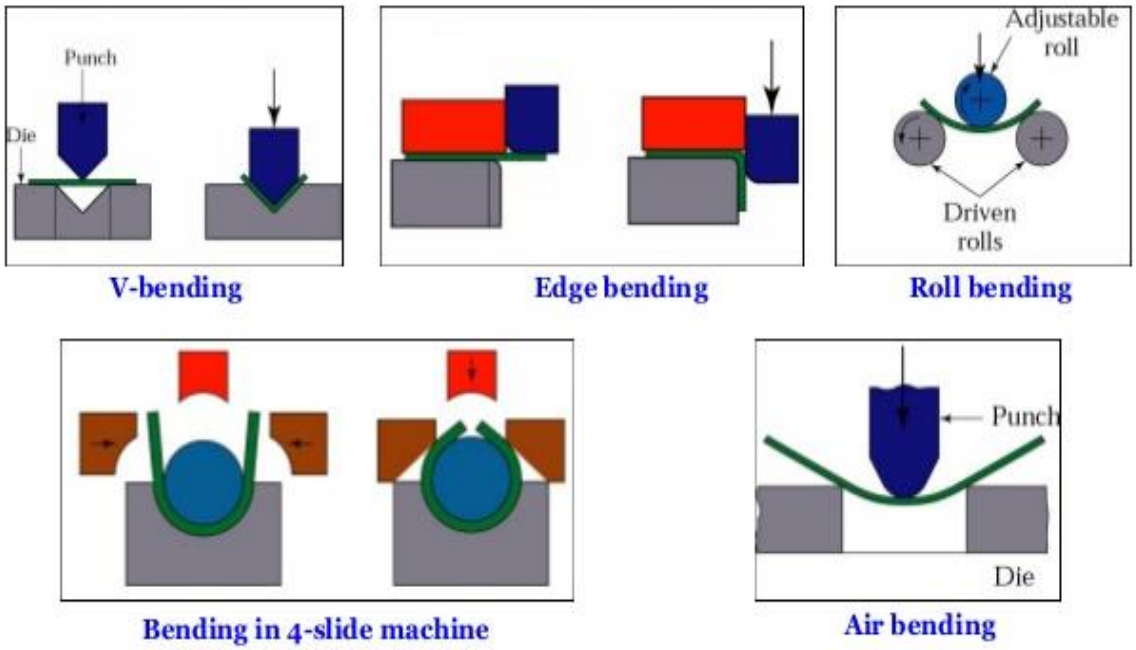

Fig 1.7 schematic representation of bending process [20]

1.3Simulation of metal forming processes

To develop and improve numerical algorithms and modeling guidelines that will allow the industry to meet its requirements in the accuracy of spring back prediction in sheet metal forming, four different problems in the metal forming and its behavior has been analyzed by Improvement of Springback Prediction in Sheet Metal Forming. [21]. And the solution for this has been discussed are as follows. In this the general outlines are

FE simulations with shell elements are used to show the negative influence of poor blank and tool discretization on the accuracy of springback prediction.

Reasons behind the error of springback prediction resulting from using standard through-thickness integration schemes for shell elements are investigated. An efficient strategy for adaptive through-thickness integration is presented and its potential is shown using academic test problems.

Several academic tests and a benchmark problem are used to evaluate the performance of a generally applicable adaptive scheme and to demonstrate the advantages of adaptive integration in FE analysis of springback in sheet metal forming.

To find the springback, the most popular experiment is U-bending, V-bending and flanging are conducted. These are the procedures where the measurement of springback can be easily identified. The major drawback of these experiments is that they cannot imitate realistic process conditions during sheet metal forming. In this procedure the punch is which is in the form of U-shape and V-shape punch will be pressed the sheet metal into the die. The results are analyzed and discussed. Stretch bending tests are used to study the importance of tension in minimizing and controlling springback. A metallic strip is fixed between the tools and is deformed by displacing the semi-cylindrical. Punch through a certain distance. Draw beads are employed to restrain the material flow. A draw bead can be considered as the local control mechanism that sufficiently restrains the material flow at relatively low blank holder force. The restraining force is created by cyclic bending and unbending the material when it travels through the draw bead. This type of test can be used to show the effect of in-plane tension on the amount of springback.

A simple bending-reverse bending experimental the experimental procedure consists of several steps: bending, turning the sheet specimen and bending in the opposite direction, turning the specimen again and bending it in the original direction, and so on. Angle after springback is determined by the coordinate measuring machine and the dependence of the angle on the deformation history can then easily be observed. The draw bending test is often used to assess springback in sheet metals under more realistic

forming conditions. During forming, the blank material experiences stretching, bending and unbending deformations when it passes the tool radius. This deformation path creates a complex stress state which is responsible for the formation of so-called sidewall curl. The major drawback of the draw bending test is the lack of control or direct measurement of sheet tension, which makes the experimental procedure less suitable for verifying the results of simulations. Then after the experiments the finite element analysis are done.

The author [21] concluded that the change of shape of the formed part is mainly caused by the relief of internal stresses developed during the deformation, hence, all factors that govern the evolution of the stress state in sheet material have a direct influence on the amount of springback. Springback dependency on some material and process parameters was demonstrated with the help of a simple analytical model The presented analytical model can be used to predict the change of curvature in the elastic-plastic sheet in the case of plane strain bending under tension It was emphasized that for an accurate springback prediction, it may be required to use a material model which can take into account the inelastic effects that occur during unloading. Based on the simulations of two benchmark problems it was demonstrated that the numerical model must reflect the physical contact conditions that exist during the stamping process. Simplifying assumptions and the uncertainty with the parameters of equivalent draw beads make the numerical model unreliable for the accurate analysis of springback. When retracting the tools after forming, contact forces are present. By combining the algorithms of the strategy, a generally applicable adaptive integration scheme was formulated and implemented in an implicit FE code between the tools and the blank. Only a few points are needed for the accurate prediction of springback in deformation regimes that produce no elastic plastic interfaces. When comes to another author, presently, for this many automobile industries tried for the composites and many other materials like aluminous and many more. To study the Characterization of the transitions between tension and out-of-plane shear crack opening modes are analyzed by failure by fracture in bulk metal forming paper had been selected.[22] The first generation AHSS are Dual Phase (DP), Complex Phase (CP) and Transformation Induced Plasticity (TRIP) steels. These steels have an ultimate strength of 600–800 MPa and total elongation of 20-25%. They are being used in automotive applications due to their good crash energy absorption capabilities and moderate strength. The second generation AHSS are Twinning Induced Plasticity (TWIP) steels, lightweight Induced-Plasticity (L-IP) and austenitic stainless steels which have a very high ultimate strength of 1200–1500 Mpa and elongation of 55-70%.[10] However, their cost effectiveness for automotive applications is very poor. Steel industries have recently developed

third generation steels, Quenched and Partitioned (Q&P) steels, which fall between the first and second generation steels, having an ultimate strength of 900–1100 Mpa and elongation of 15-18%.

Two AHSS from the first generation (TRIP) and third generation (Q&P) are selected for formability analysis. In this thesis work, they showed the caparison of the formability of both the AHSS since the phases and chemical compositions are almost similar. In this work they strain path diagrams were constructed and simulation using FEM analysis.

To understand the behavior of Q&P and TRIP steels the different tests like tensile tests (room temperature). Work hardened experiment 'n' and strength coefficient 'K' were calculated from the tensile data true stress and true strains curve are plotted.

According to this, after conducting the different experiments the conclusion of the of this work is FLC-based on proposed strain localization criterion, is in good agreement with the experimental FLC compared to other failure criteria and Formability of TRIP steel is higher compared to Q&P steels.

Formability analysis of first generation TRIP steel and third generation Q&P steel was performed by experimental and simulation methods. The following are the major conclusions from the above study.

To understand the material behavior modeling has great influence on the design of process, tools and the final product is analyzed by Incorporation of material behavior in modeling of metal forming and machining processes. [23] Material behavior is that there is no clear cut guideline as to which material model will be suitable for the particular material and specific processing conditions. In this work the various determination of the various parameters of the material model requires well-designed experimentation. Due to limited available data on the material behavior, most of the developed models have been tested only for a limited set of materials.

In metal forming, anisotropy has been considered, but the hardening behavior of anisotropic material has not been modeled properly. It is essential for a product designer to understand the behavior of material during processing and after processing. That would help the designer to select the appropriate material and matching processing method for a particular application. Apart from the product designer, the tool designer is heavily dependent on the process modeling for avoiding a costly hit and trial experiments. "Tool development and production time have been reduced by about 50% due to the use of simulations and a further 30% reduction."

Due to its importance in product and tool design, modeling of metal forming, traditional machining, and non-traditional machining has been reviewed here from the point of view of material behavior. It is clear that the prediction capability and accuracy of a model is heavily dependent on the type of material model used. Only recently, the effort to develop microstructural-based models has been put due to stringent

product quality requirement. Due to the development of newer materials and their extensive use in design, understanding during and after processing behavior of materials has become of paramount importance to a product designer.

To understand the failure in the bulk formability from some of the research has been done and procedures are as follows, Failure by surface or internal cracking in bulk metal forming is caused by the accumulation of ductile damage within regions that are highly strained due to extensive plastic flow. Apart from special purpose processes such as the shearing of bars and bar sections, where cracks are needed to cut material, the occurrence of cracks is generally undesirable and should be prevented during process design.

To present a new and simple bulk formability test that permits the determination of limiting fracture strain pairs in three-dimensional stress loading under a wide magnitude of stress triaxiality conditions. For this work, few experiments need to conduct and are follows,

Compression test:

Mechanical and friction characterization of the aluminum AA2030-T4. Stress–strain curve obtained by compression tests and detail of the cylindrical test specimen experimental measurements and ring test calibration curves relating the changes of the minimum internal diameter with the reduction in height for several friction factors.

Bulk formability test:

The bulk formability, the tests were performed on the same hydraulic testing machine as used for the mechanical and friction characterization. The work plan made use of two different groups of specimens and tool setups. The first group corresponds to conventional bulk formability tests performed with axially-loaded cylindrical specimens, cylindrical specimens loaded across a diameter (rotated cylindrical or 'Brazilian'), tapered and flanged test specimens that were compressed between flat parallel plates.

The second group corresponds to the new proposed bulk formability test that allows characterizing, fracture strain pairs in three-dimensional stress loading under varying magnitudes of stress triaxiality. The punch was made of cold working tool steel (120WV4-DIN) hardened and tempered to a Rockwell hardness. The specimens were machined from the supplied aluminum AA2030-T4 rods. And then the finite element analysis are done.

Then the author[7] concluded that the is Failure by a fracture in bulk metal forming has been analyzed by combining the fundamental concepts of plasticity, ductile damage and crack opening modes of fracture mechanics. Experiments with aluminum combined with finite element modeling and analysis

of the fracture surfaces gave the information about the bilinear fracture transitions between the tension and out of plane shear opening modes as the crack propagates from the outside surface towards the inside volume of the specimens.

1.4Forming Limited Diagram

Failure limit criterion is used to study the up which material can be safely deformed without necking or fracture. The forming limit diagram (FLD) is the most commonly used failure limit criterion in sheet metal forming industries.

A forming limit diagram (FLD) is a diagram containing measured major/minor strain points on a formed part. An FLD can distinguish between safe and necked, or failed, points. The transition from safe to failed points is defined by the forming-limit curve. [13]

FLD is a diagram of major and minor strains at the onset of local necking, schematically shown in Figure (1.8). In figure (1.9) represents the loading zone and the deep drawing part what are located in the different points. There are two types of the neck can be visible during the tensile test that are diffuse localized types of necks. When the maximum force is reached diffuse neck can be observed. It I generally observed in the width direction of the specimen. But the localized neck is formed in the thickness direction and very close to fracture.

The forming limit curve (FLC) generally represents localized necking at various strain ratios. Localized neck is highly influenced by strain rate sensitivity exponent (m) of the material. The strain rate in the neck region increases once the neck is formed.

The concept of FLD was first introduced by Keeler and Backofen3 and Goodwin.4. The FLC can be divided into two branches that are ‘‘left branch’’ and ‘‘right branch.’’ Keeler and Backofen first introduced the ‘‘right branch’’ of FLC, which is valid for positive major and minor strains. Goodwin completed the FLC by introducing the ‘‘left branch’’ of FLC, which is applicable for positive major and negative minor strains. After that, many theoretical models were developed to calculate FLD. Three different types of models are available to compute FLD: [13]

(1) The bifurcation method: bifurcation analysis was first introduced by Hill to expect diffuse necking on a metal sheet, Sto¨ ren and Rice introduced a pointed vertex on yield surface to compute FLC, and Hutchinson et al.7,8 carried out localized-band bifurcation analysis to predict FLC.

(2) Geometrical imperfection: Marciniak and Kuczynski (M–K) 9 approach that predicts instability of sheet by considering geometrical imperfection in terms of thickness difference.

(3) Damage mechanics-based approach: Chow et al.10 conducted computer simulation to analyze the effects of plastic damage on the formability of very ductile interstitial-free (IF) steel under both proportional and no proportional loading conditions.

The M–K model considered geometrical inhomogeneity as a variation of the sheet thickness directed along the minimum principal stress axis. It was assumed that during the biaxial straining, the strain localization occurs in the region of geometric inhomogeneity of the sheet. The M–K model computes limit strain using von Mises yield criteria and is underestimated in the domain of plane strain and overestimated in the domain of biaxial straining. Use of the yield criterion in the M–K model has the strong influence on the shape and position of FLC. The shape and size of geometrical imperfection (thickness ratio, width, and the angel of an imperfect region) also have great influence on the shape and position of FLC. As a result, for different thickness ratios, different FLCs can be achieved.

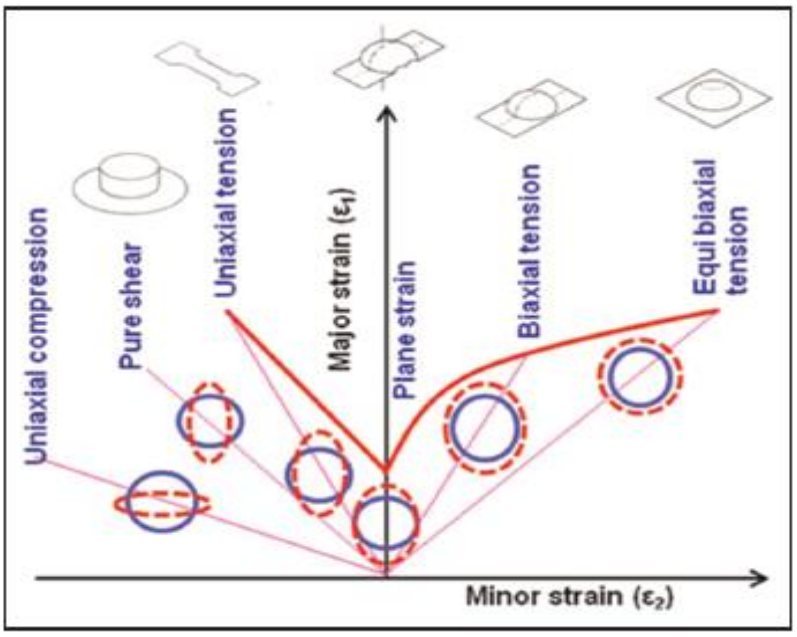

Fig 1.8 Typical FLD curves for the different deformation [14]

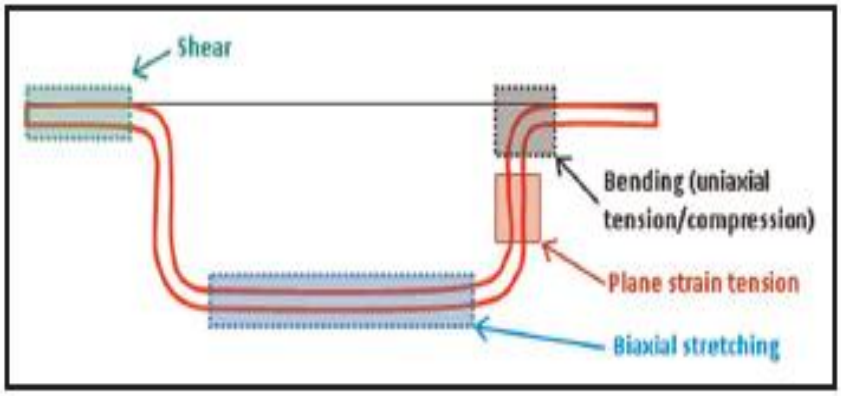

Fig 1.9 Schematic of individual loading zones of a deep drawn part.[14]

The formability of sheet metal is often calculated by using a forming limit diagram, FLD. A fracture limit curve (FLC) is plotted that shows maximum strain at fracture for different surface strain ratios.

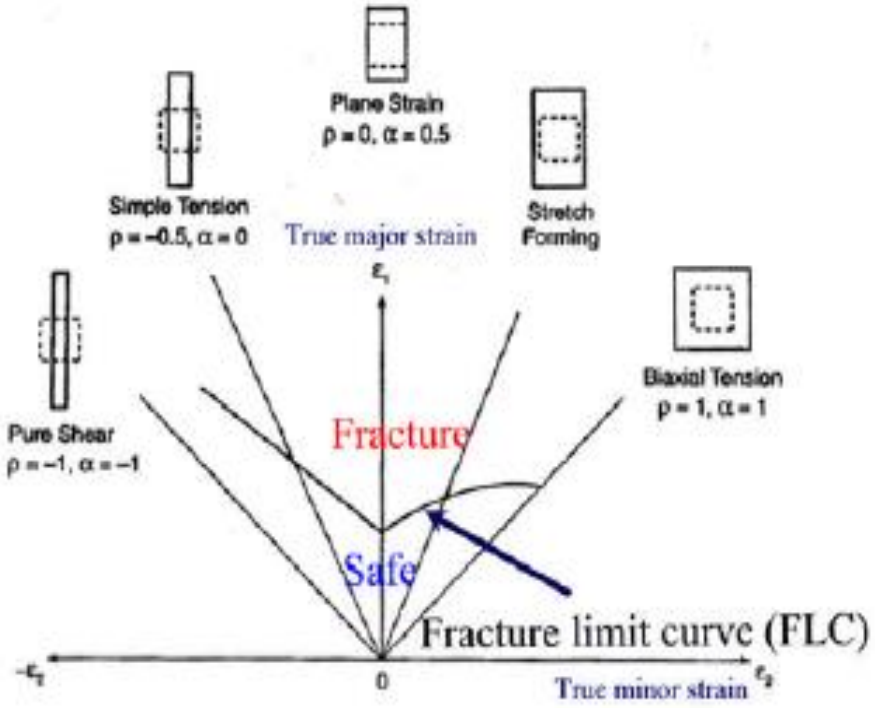

Fig 1.10 Typical FLD curves for the different deformation [14]

Under biaxial stress, below curve represents the boundary between the strain combinations that creates the fracture and those that are allowable in forming operations, shown in below fig. (1.10)

2. Experimental and numerical methodology of metal forming processes analysis

2.1 Tension test

The tension test has been performed according standard ISO 6892-1:2009 (Metallic materials - Tensile testing - Part 1: Method of test at room temperature). The quasi-static axial tension tests were run on the universal electro mechanic 50 kN tension-compression testing machine, The axial load was applied through flat manual wedge grips. Crosshead speed was approximately 20 mm/min.

Fig 2.1 Tension test.

A specimen of width of 19mm and 0.8 mm in thickness has been taken for the tension test, a tensile load is applied continuously to the specimen until the specimen fractures. During the test, the load essential to make a certain elongation on the material is recorded. A load elongation curve is plotted, so that the tensile behavior of the material can be achieved. An engineering stress-strain curve can be constructed from this load-elongation curve by making the required calculations.

Mechanical properties of selected steel. A specimen be placed in tension testing machine. As the axial load is slowly increased in increases, the total elongation over the gauge length is measured at each interval of the load and this is continued up to failure of the specimen takes place. Knowing the original cross-sectional area and length of the specimen, the normal stress σ and the strain ε can be found. The graph of these quantities with the stress σ along the y-axis and the strain ε along the x-axis. The stress-

strain diagram differs in form for various materials. The fig 2.2 shows the stress strain curve for the 6 specimens.

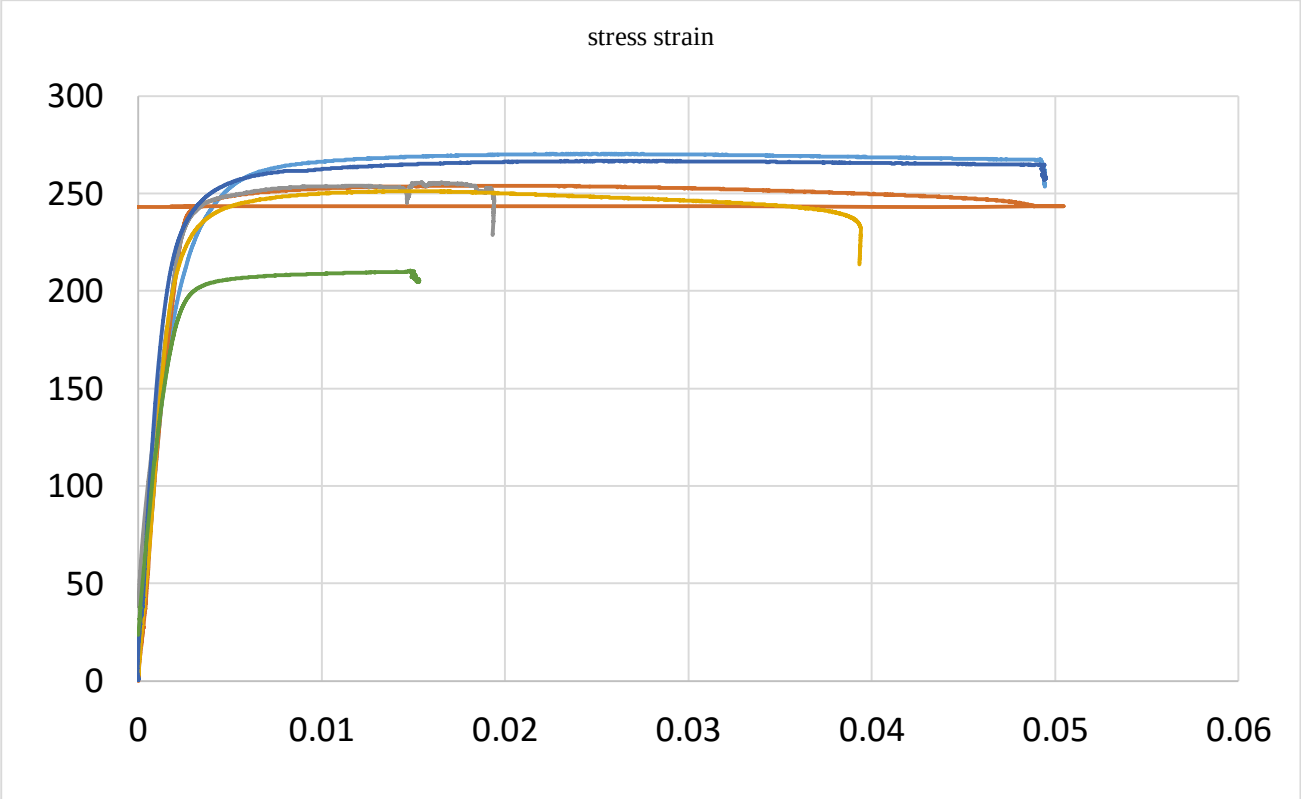

Fig: 2.2 Engineering stress strain curves for 6 specimens.

For the tension test experiment 6 specimens have been chosen with the same material. Graph 2.3 represents the 5th specimen material properties.From the fig 2.3 the grey line represents the engineering stress strain curve and the blue line indicates the true stress strain curve. Grey color line indicates the engineering stress strain curve, orange line the curve from the power law. Yellow line indicates the linear plasticity stress strain curve. 5th specimen has been chosen for the simulation in FEM method.

Specimen	1st	2nd	3rd	4th	5th	6th
Initial area mm2	16.6	14.4	14.96	15.6	15.44	14.96
Necking area mm2	5.52	7.15	7	7.15	7.25	7.5

σ y, MPa	249	248.4	249.2	234	209.1	233.2
Fracture force kN	4.23	4.134	4.056	4.308	3.996	4.326
σ u MPa	261.75	287.08	271.123	276.153	258.8	289.17
σ fracture MPa	325	349.6	346.2	355.8	336	321.6
ε ultimate	0.17	0.15	0.16	0.35	0.15	0.18
Etan, MPa	77.7	260.1	140.8	120.8	333.4	313

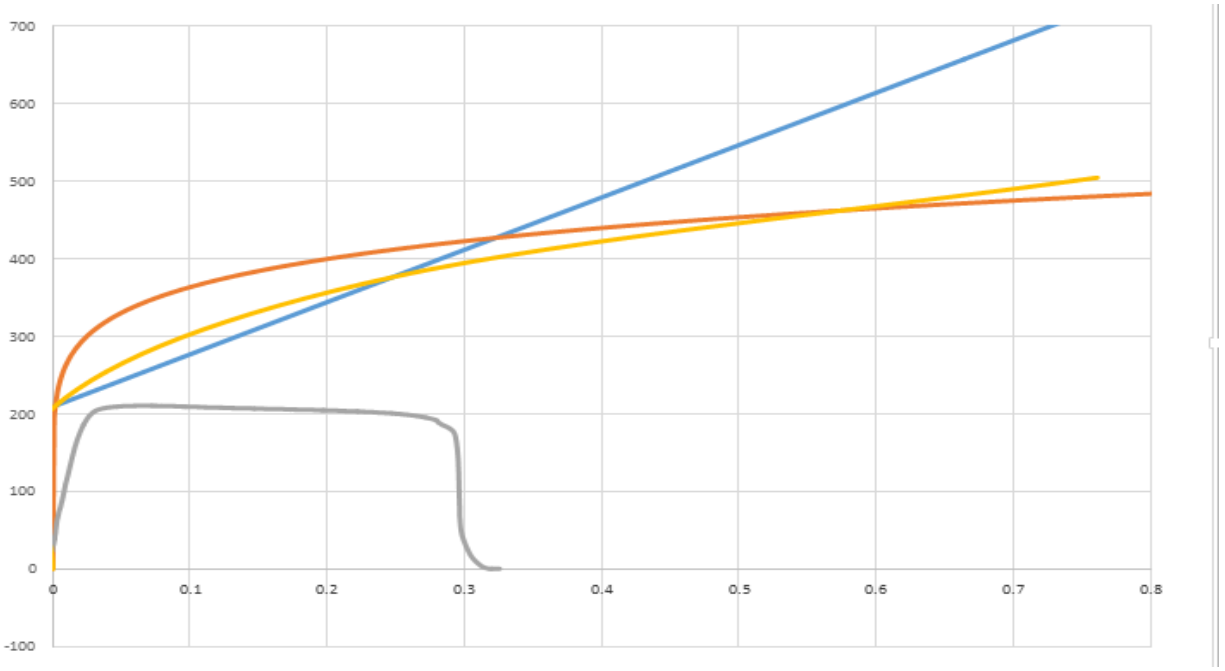

Fig: 2.3 engineering stress strain, plastic kinematic, powerlaw plasticity and true strain curve for the 5th specimen.

2.2Experimental procedure to get FLD curve

There are different approaches to get the FLD curves. The most well-known tests are given below.

1. Tensile test specimens with different notches.
2. Hydraulic tension bulge test.

3. Drag strip sheet test by hemispherical punches
4. Test by drawing with different punches shapes

- By flat punch (Marciniak)
- By hemispherical punch (Nakazim).

Hydraulic tensile test (Bulge test). We can obtain the different states of deformation using a different shapes punch at hydraulic tensile test forming as shown in the fig (2.4). Specimen preparation is very simple and greater demands are given on the creation of a large set of elliptic punches and special test equipment.

Deficiency of this test is the ability to model only states of deformations which corresponds to the Right side of FLD.

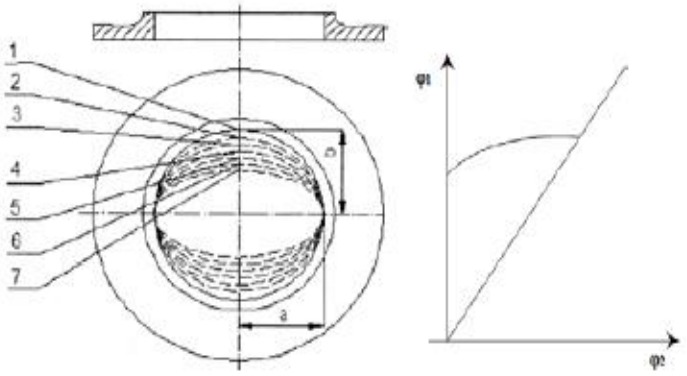

č.	1	2	3	4	5	6	7
a[mm]	50	50	50	50	50	50	50
B[mm]	50	45	40	35	30	25	20

Fig 2.4 Specimen Dimensions and the typical FLD curve for the Hydraulic tensile test[13]

The drag strip sheet test by hemispherical punches. In this process of strip sheet dragging is using already designed preparation with hemispherical punch placed on the ripper mechanism. Required different intensity distortions can be attained using a different widths of sheets strips, affecting different tensile. By stated test we can get the right and also left part of the forming limit diagram.

The right side of the diagram is typical for the deformation on punch radius or for tensile and signifies both positive deformations. The left part of the diagram shows one negative deformation, the other positive and is typical in most cases that occur on drawn part in practice.

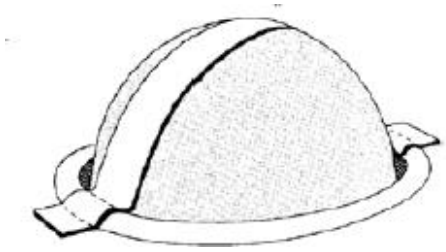

Fig 2.5 schematic representation of the drag strip test [13]

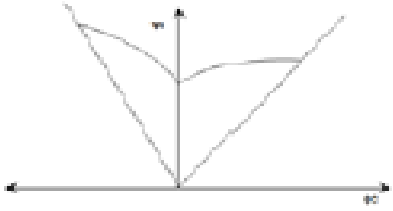

Fig Fig 2.6 typical FLD curve for the drag strip test [13]

International organization (IDDRG) for deep drawing clearly recommended the test by drawing blanks of trims which is also the most used and well-known method to determine the limit diagrams (FLD).Disadvantage of this test is in case, that straps cracking in the area of the die edge.

The test by drawing the circular plate trims with a circular derating. The test by drawing the circular plate trims with a circular derating, by hemispherical punch use the same preparation as a test with strap trims. Trims are drawn by hemispherical punch until breach of specimen. Different radius of derating and width of trims kind's difference tension positions. This method is used to acquire left and right side of forming limit diagrams. Method used seven trims by circular shape with 200 mm of radius and with derating of 20 – 80 mm as shown in the figure. Drawing used a hemispherical punch ϕ 100 mm in diameter.

FLD determined by individual methods are mutually shifted, which may be due to the geometry of the active part of the test instruments, different geometry of trim shapes, precision of measurement, materials reinforce, etc.

Fig 2.7 specimens for the Maraciniak experiment [14]

The test by drawing with different punches shapes. Punches shapes during this test can be elliptical, conical and hemispherical. The test by drawing with different punches shapes using less than the previous, as the reason for the requirement of production of solid test drawing tools of various shapes and this is time consuming and laborious.

Schematic tool representation (fixed punch) to determine the forming limit diagram deformations in the drawing tools is shown on Fig. 2.8.

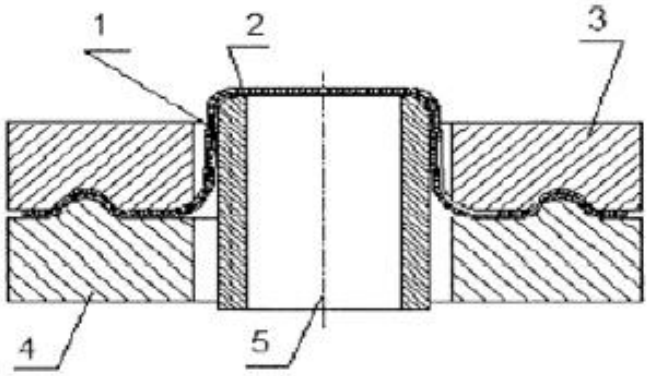

Fig 2.8 schematic representation of the Marciniak experiment [20]

Test by Marciniak scheme - sheet, 2 - pad with gap, 3 - die, 4 – blank holder, 5 – punch

Nakazima test. To get the FLD curve, tensile tests for the sheet metal will be carried out for the different dimensions of the specimens. This tension test will be carried out in the servo mechanical (instron made) tensile testing system. In this experiment a flat specimen with the particular gauge length will be tested in the certain fixed strain rate. The longitudinal and transverse strains are measured simultaneously through a video extensometer during tensile testing. . Load is measured by inbuilt load cell attached to servo mechanical tensile testing system. Engineering stress is calculated by dividing

The load with initial cross-sectional area. True stress is calculated from engineering stress by assuming the volume consistency condition. FLDs are generated by following normal Nakazima procedure.

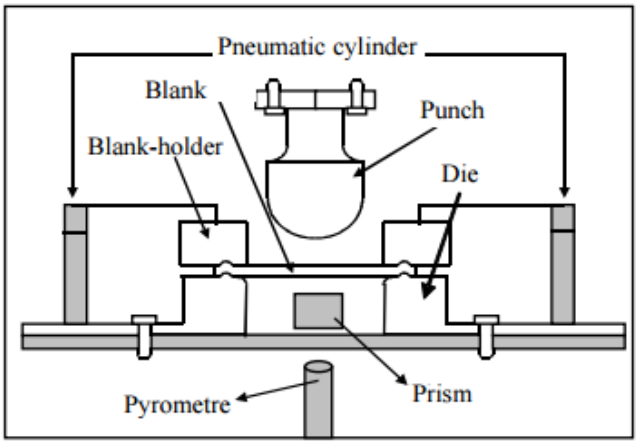

Fig 2.9Nakazima experimental instrument [19]

The Nakazima one of the usual experimental tests which provides the information on formability of sheet material. Nakazima is much simpler to perform. The Nakazima set-up is made of a hemispherical punch, a die, a blank-holder and a draw-bead which prevents any sliding motion. Several sensor data are recorded during the test, such as the punch load and local temperature histories. A grid is etched on the blank and allows determining the strain distribution by a posteriori analysis using pattern recognition systems. And it is possible to vary several parameters of the blank and of the tool. In this various strains are generated by varying the width of the sample. All samples length is fixed but varying in the width of the samples.[21]

Fig 2.10 specimens for the Nakazima experiment.[14]

The experimental procedure to determine FLD involves three stages, grid marking on the sheet specimens, onset of localized necking, and measurement of strains. The circles on the sheet samples became ellipses after deformation, falling into safe, necked, wrinkled and failed zones. Finally, FLD is drawn by plotting the minor strain and the corresponding major strain along the ordinate and by drawing a curve that separates the safe region from the unsafe region. After experimentation, center-to-center distances of the dots become altered in the rolling and perpendicular to the rolling directions, one direction becoming higher in comparison with the other. This center-to-center distance of the dots is used to calculate major and minor strains. Finally, the FLC is then drawn clearly defining the safe limiting strains from the unsafe zone containing the necked and fractured zones.

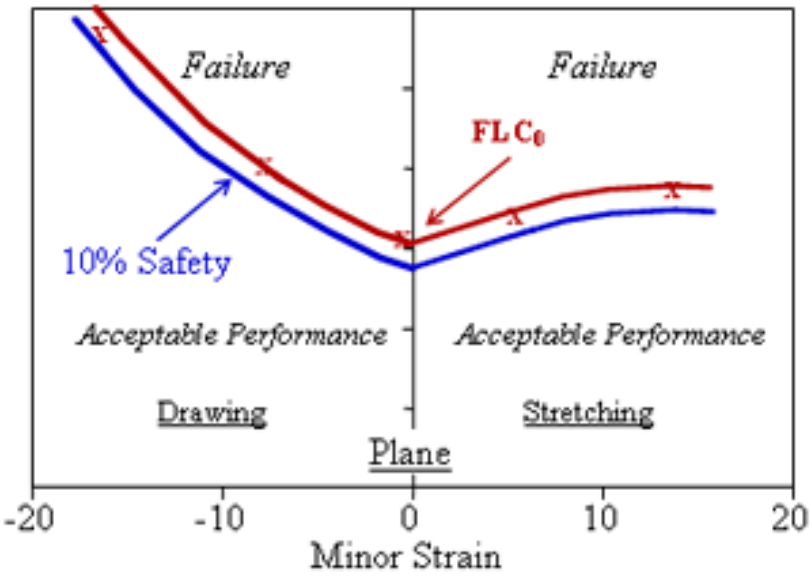

Fig 2.11 FLD typical curve [13]

2.3FLD curve from empirical formula

FLC0 is one of the most important parameter in the FLC. FLC0 is the major principal strain at the onset of necking at plane strain condition. The parameter FLC0 is usually defined from empirical formula. An experimental formula is used to determine FLC0 in a wide range of steels as proposed by Keeler and Brazie.[14]

$$FLCo = Ln\left[1 + \frac{13.3+14.03t}{100}\right]^{\frac{n}{0.21}} \quad \text{For } n \leq 0.21 \qquad (2.1)$$

$$\begin{cases} \in \varepsilon < 0, \varepsilon_1 = \mathrm{FLCo} - \varepsilon_2 \\ \varepsilon_2 = 0, \mathrm{FLCo} = \mathrm{Ln}\left[1 + \frac{13.3+14.03t}{100}\right]^{\frac{n}{0.21}} \\ \varepsilon_2 > 0, \varepsilon_1 = (1 + \mathrm{FLCo})(1 + \varepsilon_2)^{0.5} - 1 \end{cases} \quad (2.2)$$

Where t is the sheet thickness measured in millimeters and n is the strain hardening exponent in power law expression. In the above formula, FLC0 is represented in true strain. The full FLC can be calculated from equation given above, by considering isotropic von Mises yield criteria where ε_2 and ε_1 are the true minor strain and major strain.

2.4Introduction of LS DYNA

The developers of LS-DYNA is LSTC (Livermore Software Technology Corp.), LS-DYNA is a general purpose temporary dynamic finite element program capable of simulating compound real world problems. LS-DYNA is a combined explicit/implicit solver. The program was initially designed for extremely transient dynamics FEA, using explicit time integration. Transient dynamics, mentions to events with high speed and short time where inertial forces are vital. The implicit solver was first implemented in 1998 and is still being developed. LS-DYNA is primarily used, for its fast explicit solver, in nonlinear problems with large deformations, such as, predicting a car's behavior in a collision. The following analysis capabilities are available in LS-DYNA [2].

- Nonlinear dynamics
- Rigid body dynamics
- Quasi-static simulations
- Normal modes
- Linear statics
- Fluid analysis
- FEM-rigid multi-body dynamics coupling
- Underwater shock
- Failure analysis
- Crack propagation
- Real-time acoustics
- Design optimization

- Implicit springback
- Multi-physics coupling
- Structural-thermal coupling
- Adaptive Remeshing

Advantages of using LS-DYNA for limit load analysis. The main advantage of LS-DYNA in limit load analysis is the nonexistence of convergence problems essential to the solution algorithm. Not even arbitrary contact surfaces cause problems. Due to status fluctuations in contact the contact forces might fluctuate sometimes. This would deteriorate convergence significantly in an implicit analysis but in LS-DYNA analyses this is of minor position. Due to small time steps amplitudes usually remain within a certain level and the averaged forces stay meaningful.

A further benefit of dynamic analysis is that in the locality of a critical point the inertia forces steady the system motion even in the post-critical range where the load which the system can transmit decreases with growing displacements. Thus, the character of the post-critical behavior can be studied.

Disadvantages of explicit transient solution in static limit load analysis. The LS-DYNA solution system is only appropriate to general transient analysis. Thus inside the solution always inertia forces, often also damping forces are involved. Thus for static respectively quasi-static analyses velocities and accelerations have to be selected in such a fashion that forces due to inertia and damping remain slightly small. Especially, initial conditions must be selected wisely to avoid fluctuations, they should match a static solution very closely and should introduce any motion very smoothly into the system.

3. Determination of FLD curve using numerical simulation

In this work, we have taken the approach with the different radius notches for the tensile test. In this similarly the determination of the mechanical properties, the specimen of different dimensions has been chosen, as shown in the figure 3.1. The preparation of the specimens are easy and it is really one of the well-known approach to get the FLD curves. Deficiency of this test is the ability to model only states of deformation which corresponds to the left side of FLD.[26]

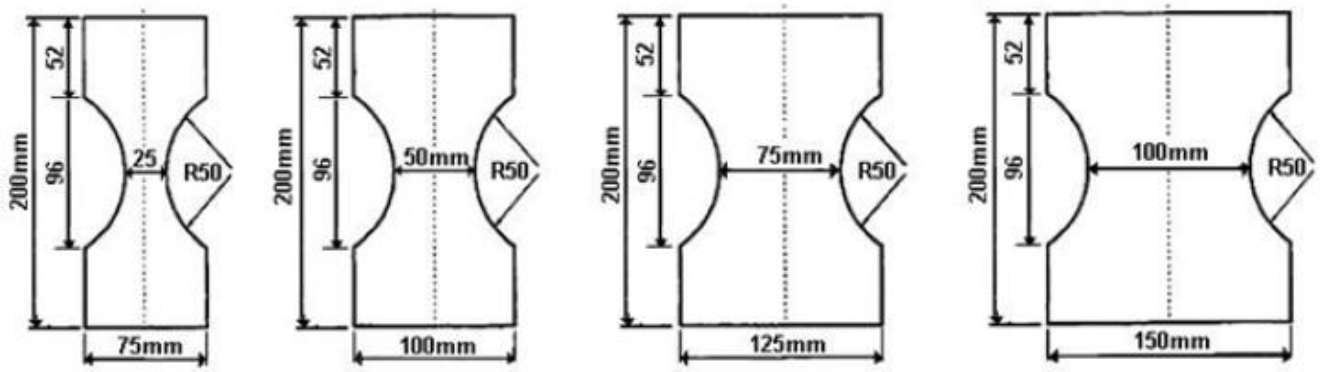

Fig 3.1 dimension of the specimen taken for the simulating the tension test and to obtain the FLD curves

A phenomenological model is proposed for the prediction of FLD from simply tensile material properties.. From the points we can say that the material behavior and up to which strain point is safe and above which strain point is unsafe. To check the validity of the proposed model, three material have been selected, they are piecewise linear plasticity and power law plasticity and plastic kinematic. Comparison with the experimental data shows that the calculated FLD can predict the sheet metal forming limits accurately.

After simulation the different materials properties in the finite element method, the following FLD curves we obtain for the all the four different specimens. The FLD curves are shown below,

Material property: linear piecewise plasticity.

Specimen width = 150mm. In the figure 3.2 shows the FEM model of the specimen. In this model the notch width is 100 mm, the radius of the notch is 50 mm and the length of the gauge length is 96mm. fig 3.2 (c) shows the FLD curve for the specimen 1. For the FEM model, for the upper most

nodes are subjected to prescribed motion set and the bottom are fixed nodes. These nodes are subjected to Spc boundary conditions. In the specimen 1 points are mentioned that are 1, 2, 3 and 4. The points 3 and 4 are subjected to more tension force when compared to 1 and 2. We could clearly see in the FLD curve. And we will get only points in the left part of the curve because of uniaxial tension. When the points crosses the FLD curve then it crosses the safe zone. Fig 3.2 b) shows the formability diagram for the part, which can gives the information about the material after deformation like severe thinning, crack propagation and so on.

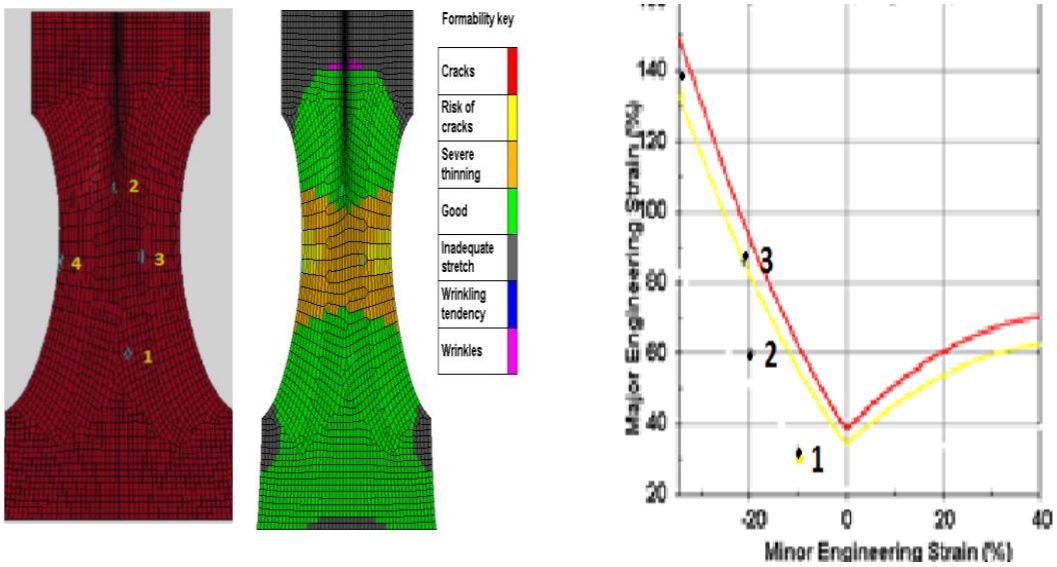

Fig 3.2 FEA results of tension test with specimen width = 150mm a) FE model of specimen, b) Formability diagram, c) FLD curve and strains at selected points

Specimen width = 125mm. In the figure 3.3 shows the FEM model of the specimen 2. In this model the notch width is 75 mm, the radius of the notch is 50 mm and the length of the gauge length is 96mm. fig 3.3 (c) shows the FLD curve for the specimen 2. In the specimen 2 points are mentioned that are 1, 2, 3 and 4. The points 3 and 4 are subjected to more tension force when compared to 1 and 2. We could clearly see in the FLD curve. Fig 3.3(b)shows the formability diagram for the specimen.

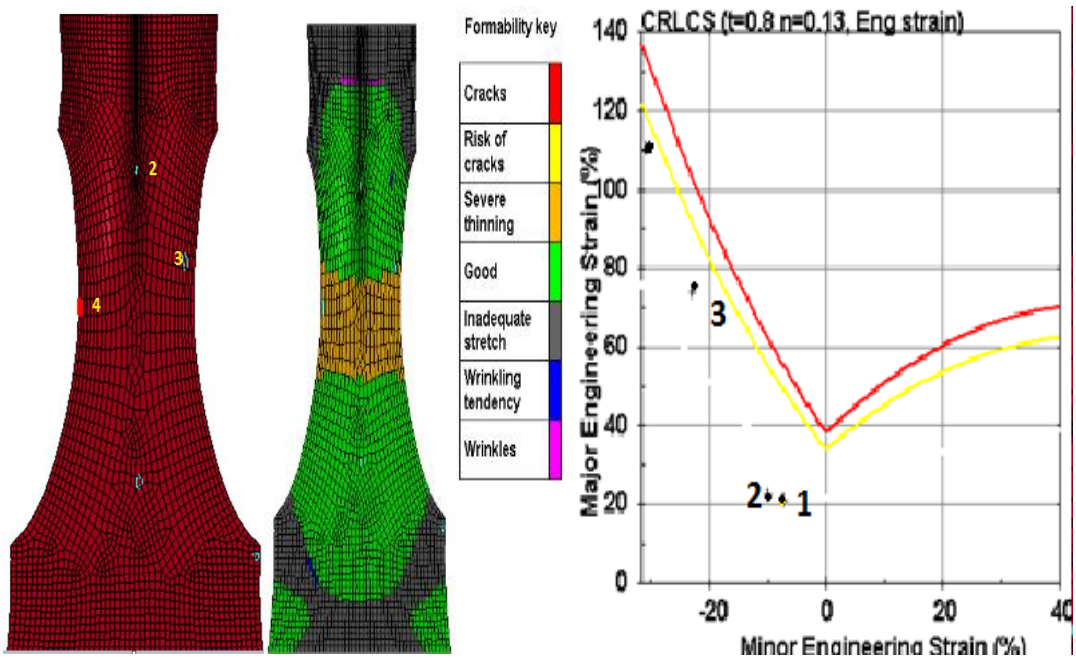

Fig 3.3 FEA results of tension test with specimen width = 125mm a) FE model of specimen, b) Formability diagram, c) FLD curve and strains at selected points

Specimen width = 100mm. In the figure 3.4 shows the FEM model of the specimen 3. In this model the notch width is 50 mm, the radius of the notch is 50 mm and the length of the gauge length is 96mm. fig 3.4 (c) shows the FLD curve for the specimen 2. In the specimen 3 points are mentioned that are 1, 2, 3 and 4. The points 3 and 4 are subjected to more tension force when compared to 1 and 2. We could clearly see in the FLD curve. Fig 3.4 (b) shows the formability diagram for the part

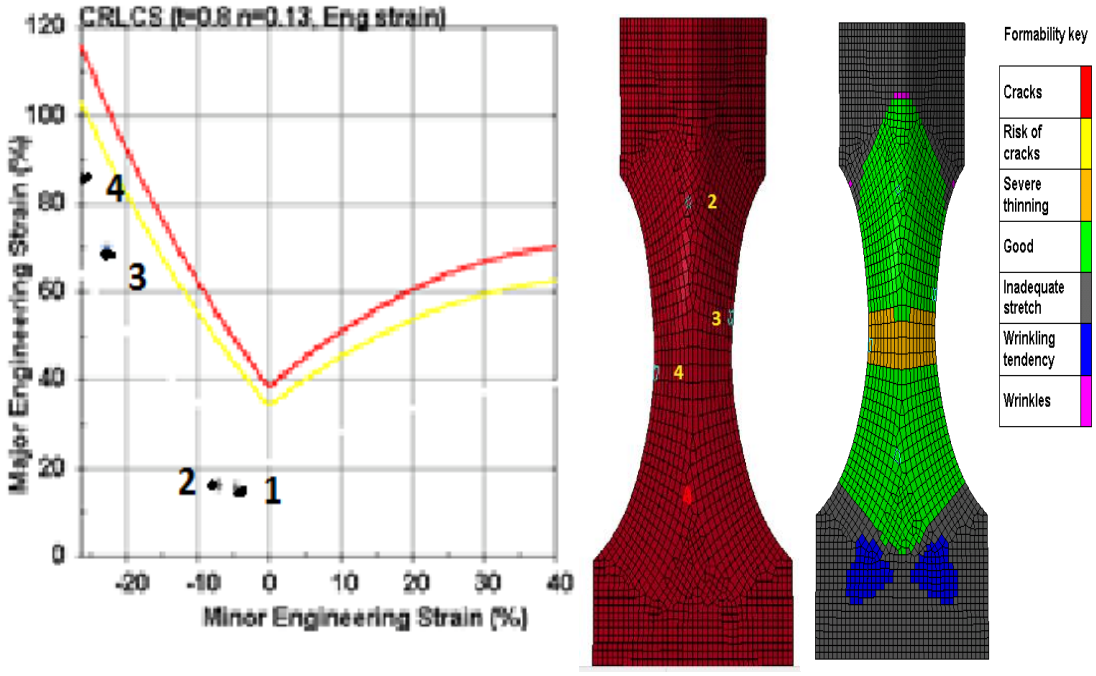

Fig 3.4 FEA results of tension test with specimen width = 100mm a) FE model of specimen, b) Formability diagram, c) FLD curve and strains at selected points

Specimen width = 75mm. In the figure 3.5 shows the FEM model of the specimen 4. In this model the notch width is 25 mm, the radius of the notch is 50 mm and the length of the gauge length is 96mm. fig 3.5 (c) shows the FLD curve for the specimen 4. In the part 4 points are mentioned that are 1, 2, 3 and 4. The points 3 and 4 are subjected to more tension force when compared to 1 and 2. We could clearly see in the FLD curve. Fig 3.4 (b)shows the formability diagram for the specimen.

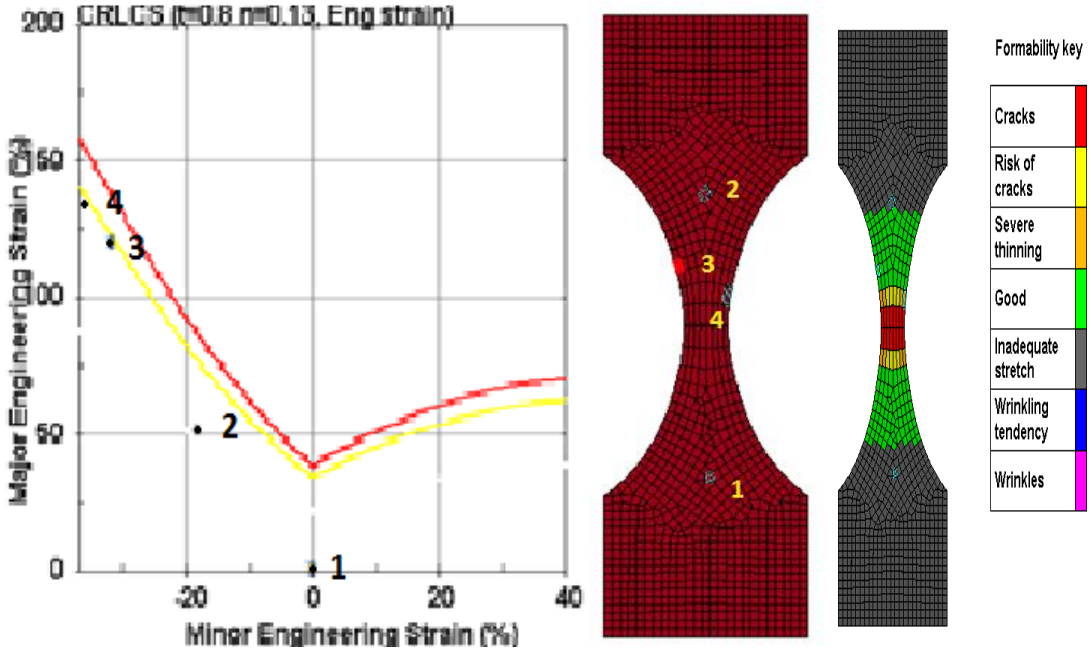

Fig 3.5 FEA results of tension test with specimen width = 75mm a) FE model of specimen, b) Formability diagram, c) FLD curve and strains at selected points

Material model: Plastic kinematic

Specimen width = 150mm. The fig 3.6(a) shows the FEM model for the material plastic kinematic. In the Specimen 1 points are mentioned that are 1,2,3 and 4. The points 3 and 4 are subjected to more tension force when compared to 1 and 2 as plotted in FLD curve. Fig 3.6(c)shows the formability diagram for the part.

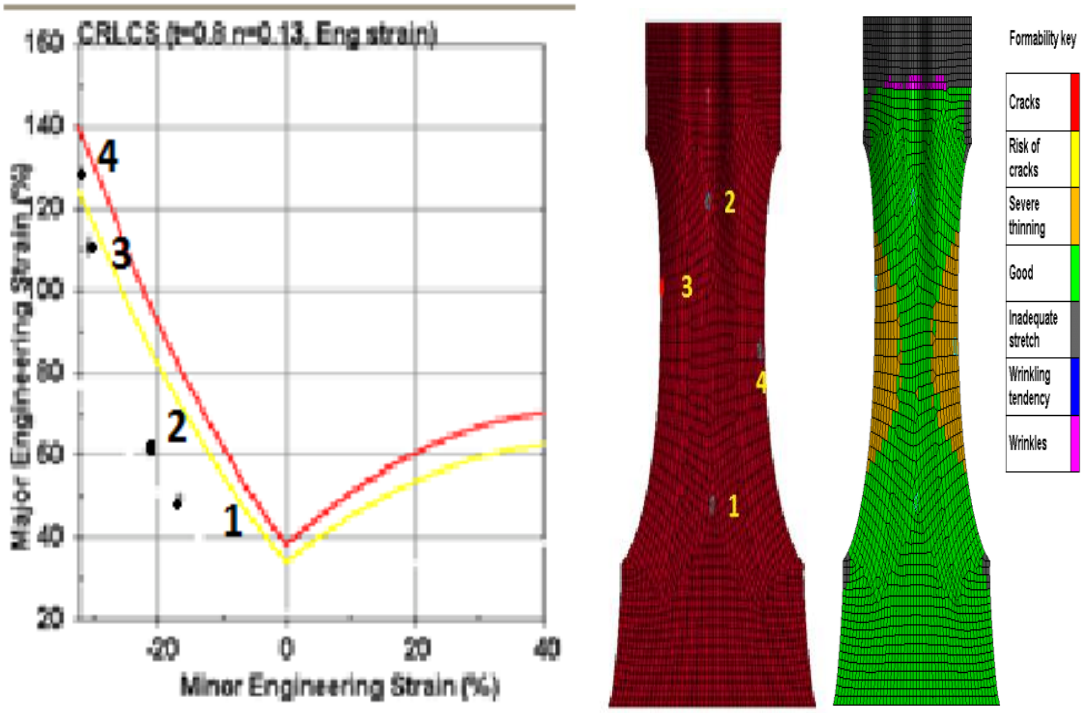

Fig 3.6 FEA results of tension test with specimen width = 150mm a) FE model of specimen, b) Formability diagram, c) FLD curve and strains at selected points

Specimen width = 125mm. The fig 3.7 shows the FEM model for the material plastic kinematic of the specimen 2. In the specimen 2 points are mentioned that are 1, 2, 3 and 4. The points 3 and 4 are subjected to more tension force when compared to 1 and 2 as plotted in FLD curve. 3.7(c) 4.27 shows the formability diagram for the part

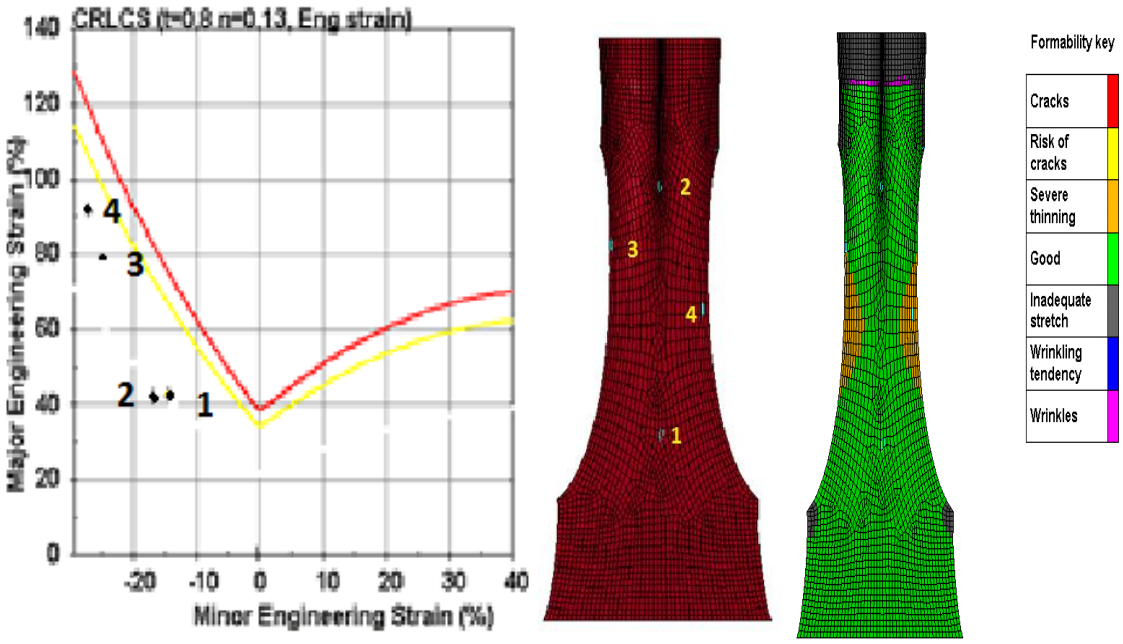

Fig 3.7 FEA results of tension test with specimen width = 150mm a) FE model of specimen, b) Formability diagram, c) FLD curve and strains at selected points

Specimen width = 100mm. The fig 3.8 shows the FEM model for the material plastic kinematic of the specimen 3. In the part 2 points are mentioned that are 1, 2, 3 and 4. The points 3 and 4 are subjected to more tension force when compared to 1 and 2 as plotted in FLD curve. Fig 3.8(c) shows the formability diagram for the part

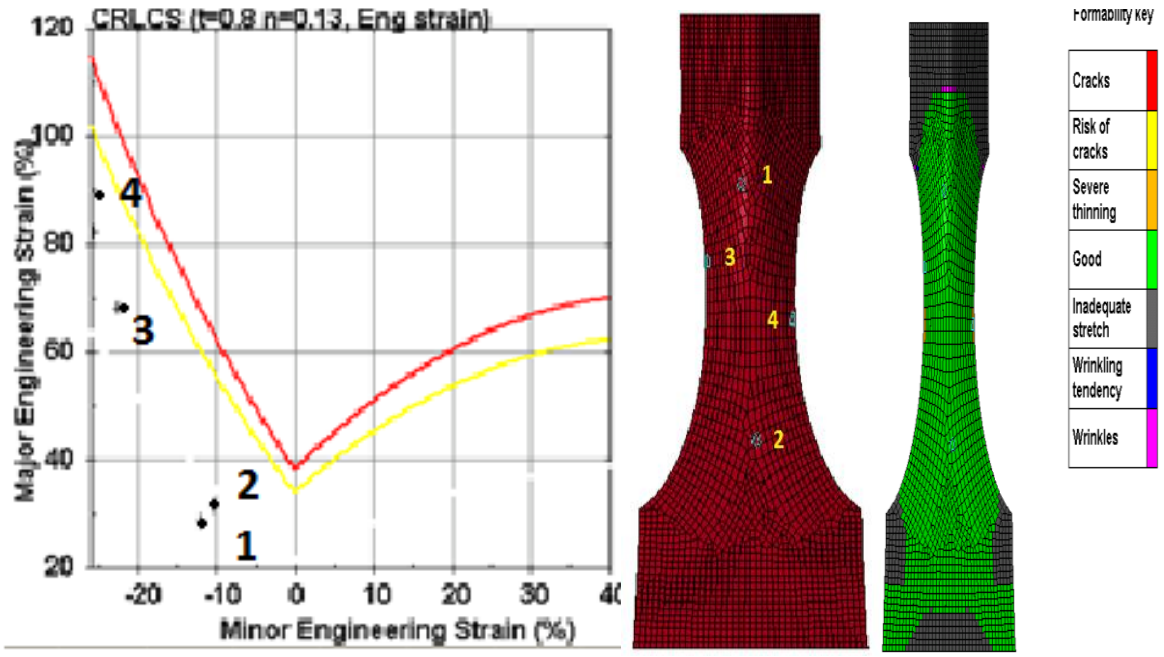

Fig 3.8 FEA results of tension test with specimen width = 150mm a) FE model of specimen, b) Formability diagram, c) FLD curve and strains at selected points

Specimen width = 75 mm. The fig 3.9 shows the FEM model for the material plastic kinematic of the specimen 4. In the part 2 points are mentioned that are 1, 2, 3 and 4. The points 3 and 4 are subjected to more tension force when compared to 1 and 2 as plotted in FLD curve. Fig 3.9(c) shows the formability diagram for the part

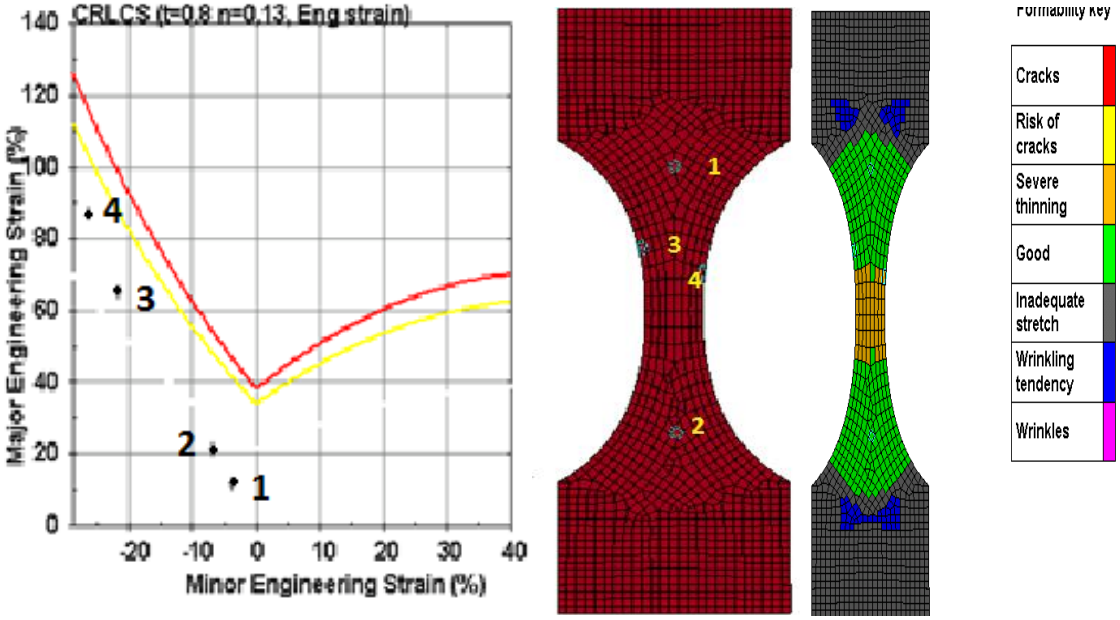

Fig 3.9 FEA results of tension test with specimen width = 150mm a) FE model of specimen, b) Formability diagram, c) FLD curve and strains at selected points

Material model: Powerlaw plasticity

Specimen width = 150mm. The fig 3.10 shows the material property for the Powerlaw Plasticity. The same dimensions of the specimen has been taken to check the behavior of the material property and plotting FLD curve. Fig 3.10(c) shows the formability diagram for the specimen. Points 4 and 3 are subjected to the more tension force when compared to the points 1 and 2 as mentioned in the FLD curve.

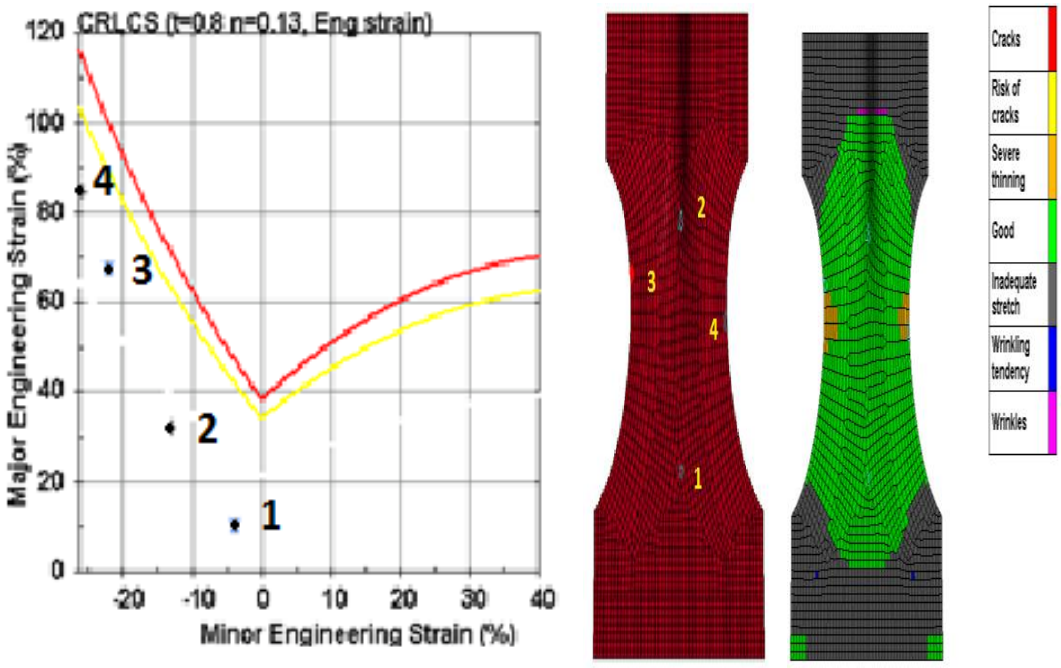

Fig 3.10 FEA results of tension test with specimen width = 150mm a) FE model of specimen, b) Formability diagram, c) FLD curve and strains at selected points

Specimen width = 125mm. The fig 3.11 shows the material property for the Powerlaw Plasticity. The same dimensions of the specimen has been taken to check the behavior of the material property and plotting FLD curve. Fig 3.11(c) shows the formability diagram for the part. Points 4 and 3 are subjected to the more tension force when compared to the points 1 and 2 as mentioned in the FLD curve.

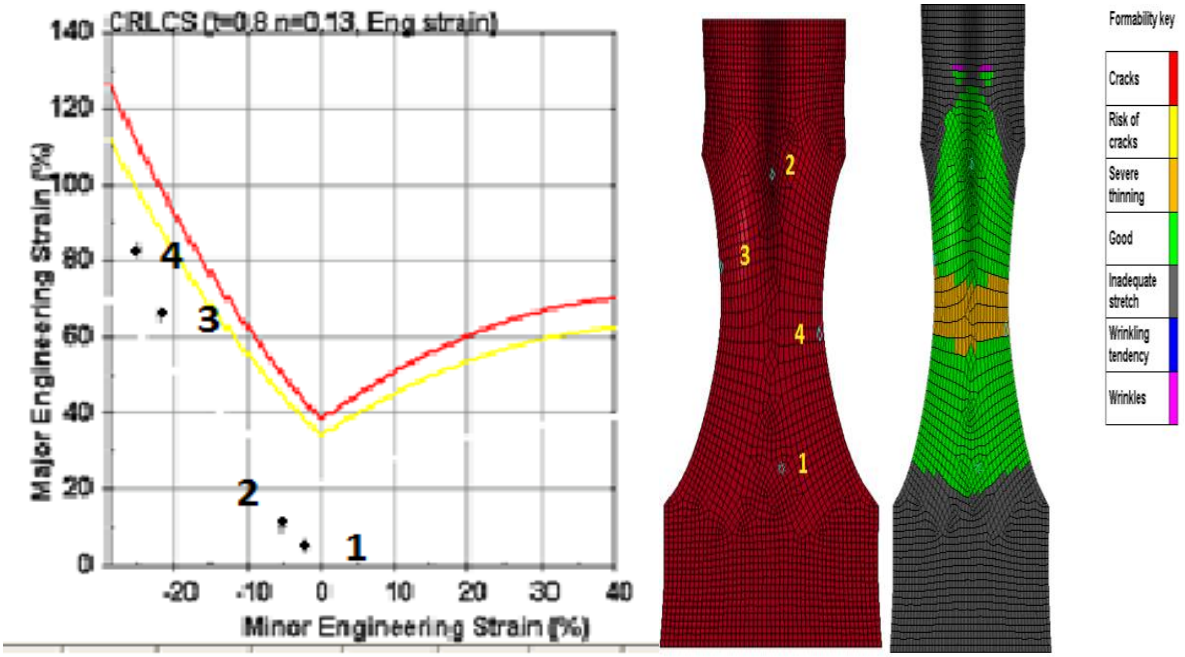

Fig 3.11 FEA results of tension test with specimen width = 150mm a) FE model of specimen, b) Formability diagram, c) FLD curve and strains at selected points

Specimen width = 100mm. The fig 3.12 shows the material property for the Powerlaw Plasticity. The same dimensions of the specimen has been taken to check the behavior of the material property and plotting FLD curve. Fig 3.12(c) shows the formability diagram for the specimen. Points 4 and 3 are subjected to the more tension force when compared to the points 1 and 2 as mentioned in the FLD curve

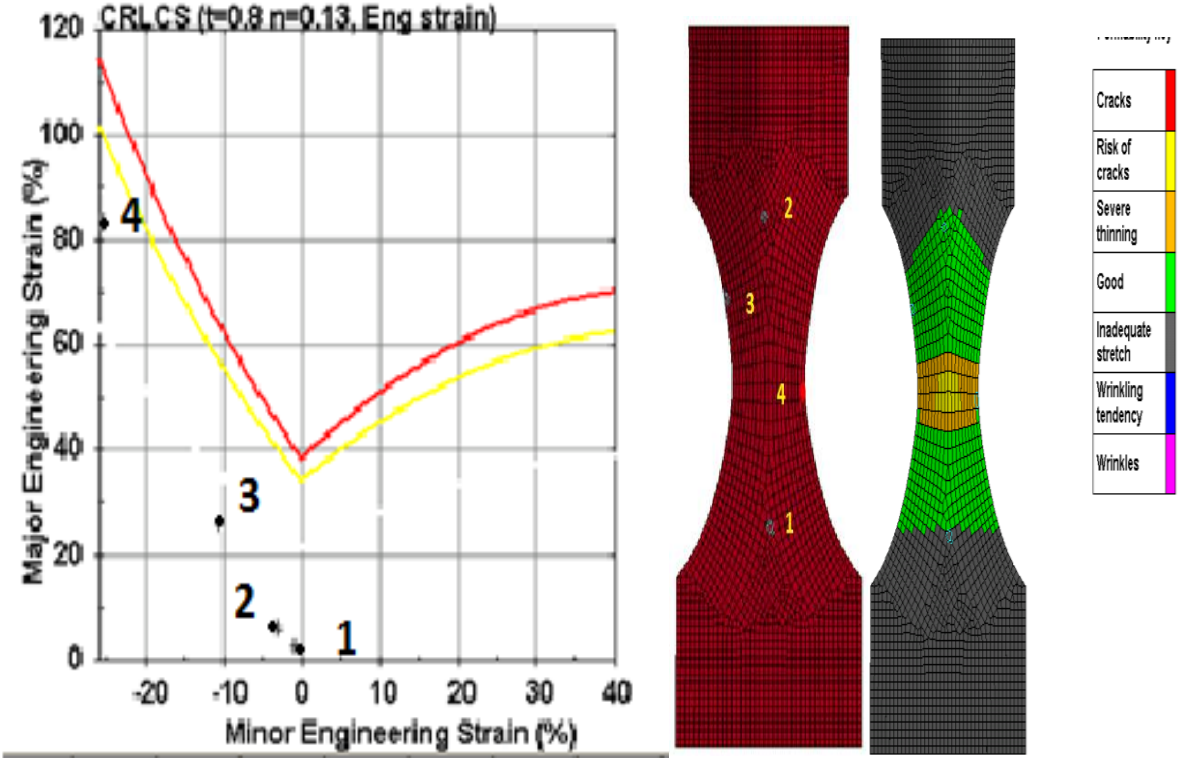

Fig 3.12 FEA results of tension test with specimen width = 150mm a) FE model of specimen, b) Formability diagram, c) FLD curve and strains at selected points

Specimen width = 75mm. The fig 3.13 shows the material property for the Powerlaw Plasticity. The same dimensions of the speciemen has been taken to check the behavior of the material property and plotting FLD curve. Fig 3.13(c) shows the formability diagram for the speciemen. Points 4 and 3 are subjected to the more tension force when compared to the points 1 and 2 as mentioned in the FLD curve.

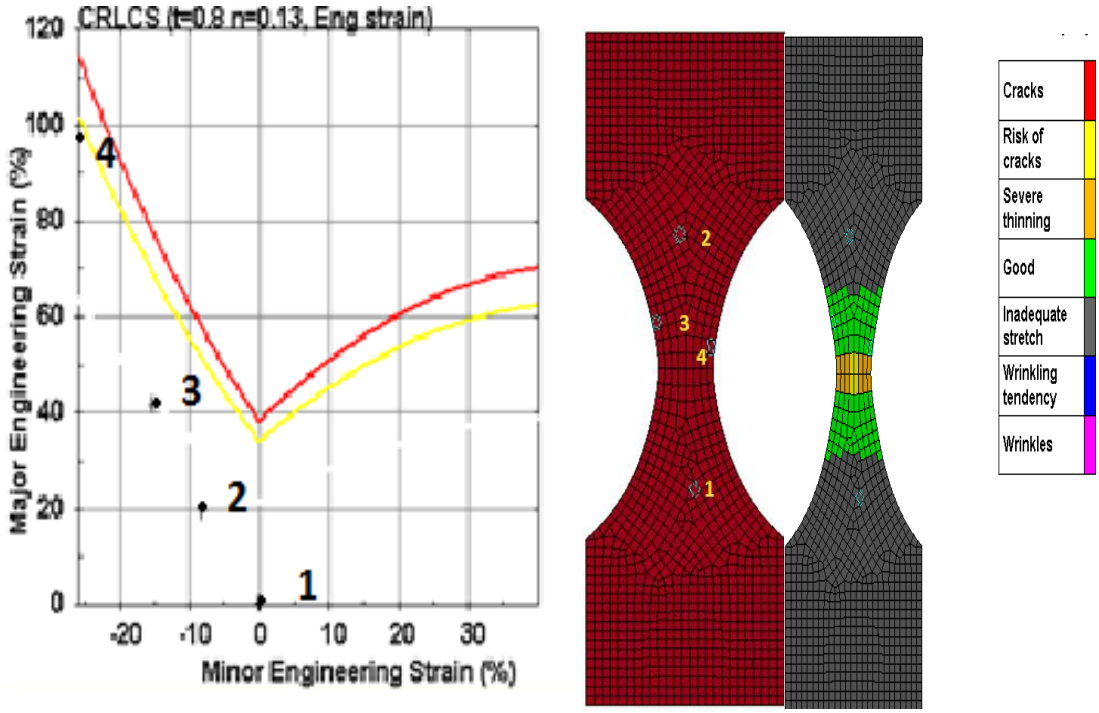

Fig 3.13 FEA results of tension test with specimen width = 150mm a) FE model of specimen, b) Formability diagram, c) FLD curve and strains at selected points

4. Cupping test

4.1Experimental methodology cupping test

Cupping test will be done with a prescribed speed limit until it results in a fine, continues in the sheet method. The displacement of spherical punch till cracking occurs is known as cupping index.

This experiment setup consists of spherical punch, drawing die, blank holder and specimen (sheet metal). In this experiment a square specimen of 64 mm and 0.8 mm in width has been taken. In this experiment the specimen will be placed in between the blank holder and drawing die. From the top the punch pushed the specimen. Specimen will be fixed firmly when the force is applied on the specimen, the specimen will start to deform and at some point the specimen fractures. From this the displacement and force will be recorded from the different sensors used in the equipment and the graph will be shown.

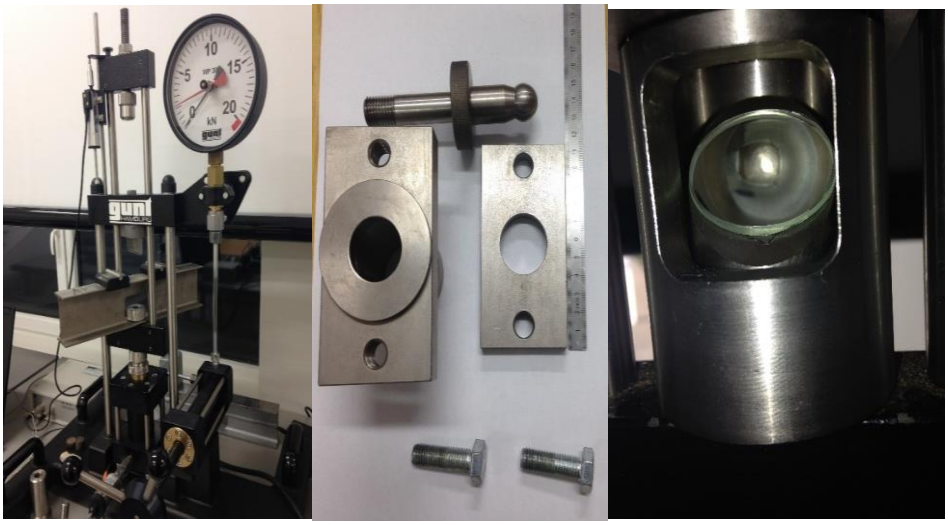

Fig 4.1 cupping test equipment and tools

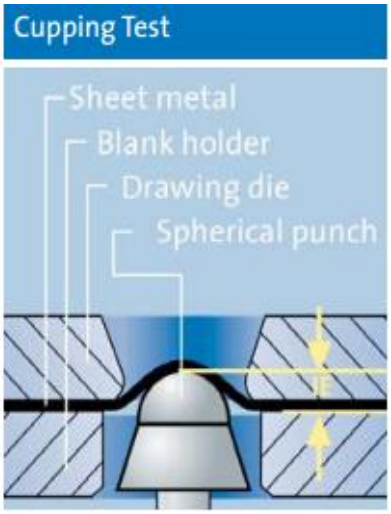

Fig 4.2 schematic diagram of cupping test experiment [3]

Fig 4.3 fracture of the specimen in cupping test experiment

4.2Simulation of cupping test

The numerical simulations of the axial crushing of longitudinal member were carried out using the non-linear explicit finite element (FE) analysis solver LS-DYNA v.970. In the FEM model the specimen is done by two mesh sizes 3mm and 0.6 mm. In the mesh size 3mm approximely 2.500 nodes and in mesh size 0.6mm approximately 12.500 nodes. The material properties basically were described by

*MAT_POWER_LAW_PLASTICITY, *MAT_LINEAR_PIECEWISE_PLASTICITY and *MAT_PLASTIC_KINEMATIC model with strain rate insensitive option in LS-DYNA FE model.

The numerical model consists of longitudinal member and two rigid upper and lower plates. The longitudinal member was assembled of cylindrical punch. The specimen is fixed between the two upper and lower plates. The specimen will be held firmly with the force of 300 kN from the plates. Then the longitudinal member will be applying the force for the specimen with the constant velocity of 1m/s. The stress strain curve will be defined by the material properties obtained from the tension test. The square specimen is of 64 mm. Longitudinal punch is made to move freely in the Z axis.

The length of the longitudinal punch is 40 mm. the force will be applied from the distance of 2mm from the specimen. The FEM model of the specimen are shown in the figure.4.4.

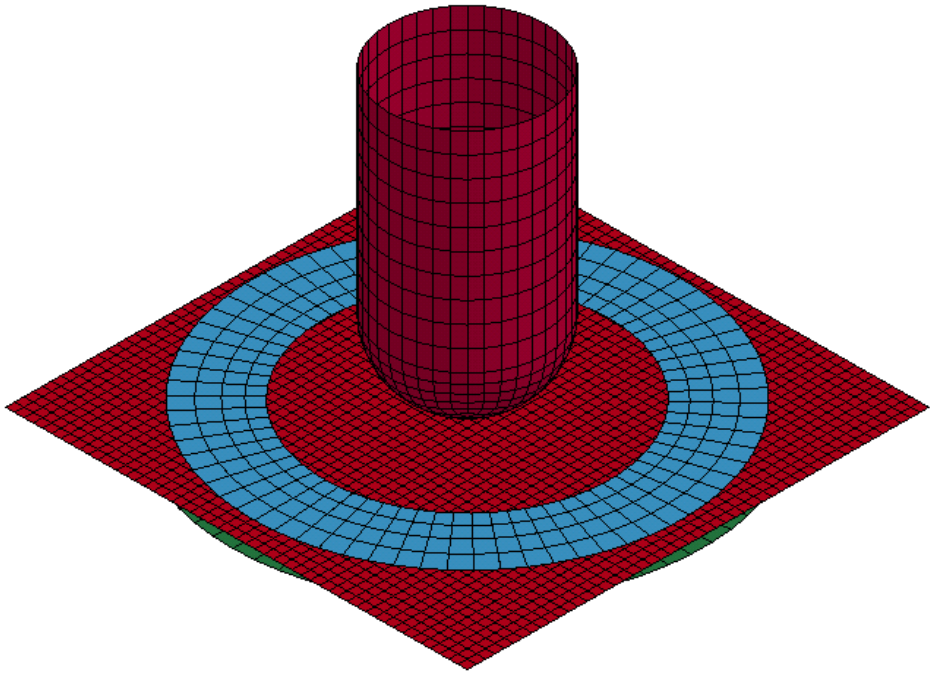

Fig 4.4 FEM model of cupping test in LS prepost

5.1 Results Material type: Powerlaw plasticity

The Fig 4.5 shows the FEM model for the cupping test. Few points on the part has been selected to get the FLD curves. In this curve we will get the points in both the sides of the curve because this is biaxial tension. In this graph, points 1, 2, 3 and 4 are shown in the FEM model. Fig 4.5(c) shows the formability diagram. Fig 4.5(d) shows the von mesis stress on the material.

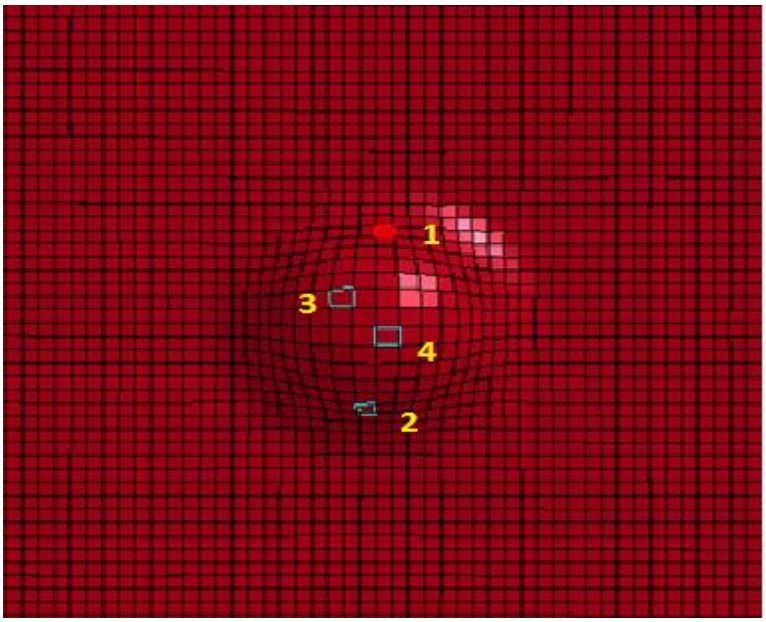

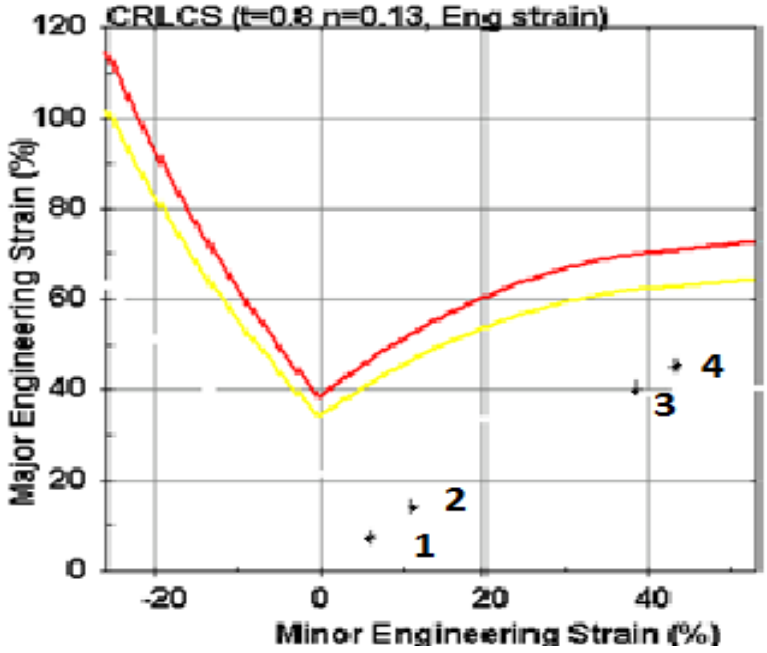

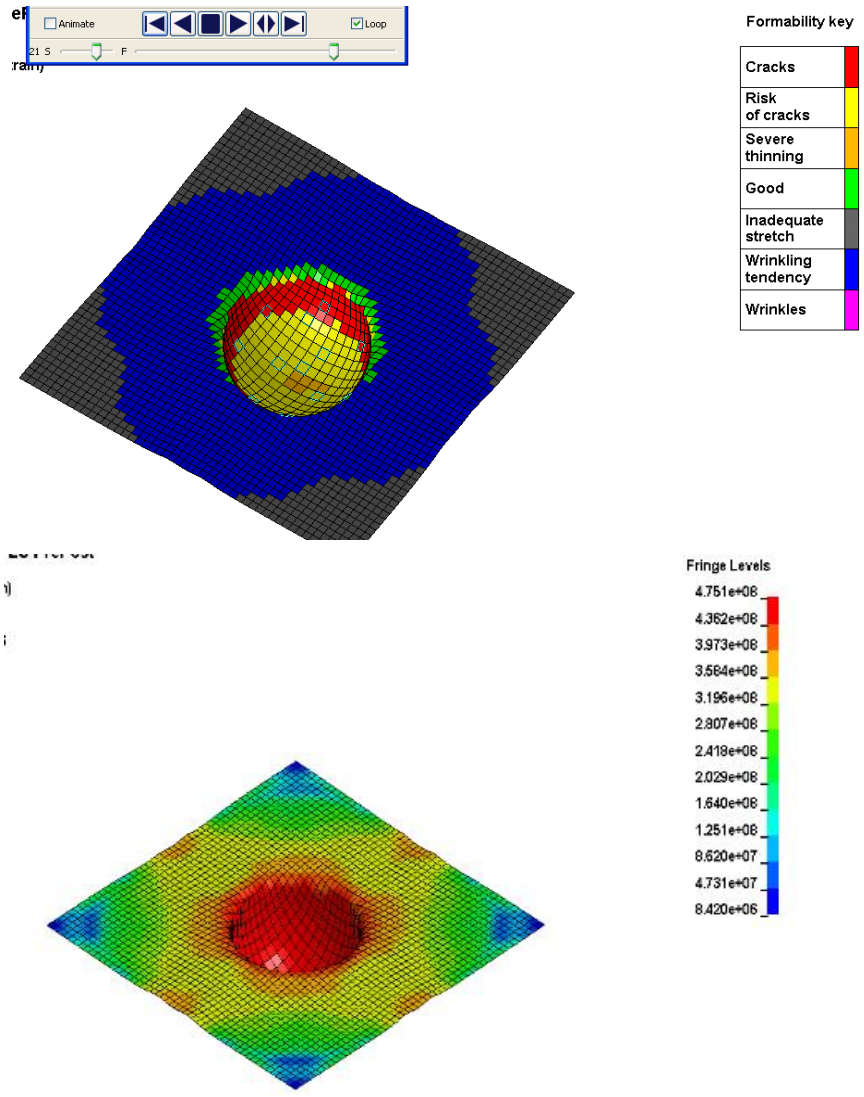

Fig 4.5 FEA results of cupping test with specimen material property powerlaw plasticity a) FE model of specimen, b) Formability diagram, c) FLD curve and strains at selected points d)Von mesis stress of the specimen

5.2 Results Material: Plastic kinematic

The Fig 4.6 shows the FEM model for the cupping test. Few points on the part has been selected to get the FLD curves. 1, 2, 3 and 4 are shown in the FEM model. Fig 4.6(c) shows the formability diagram. Fig 4.6(d)shows the von mesis stress on the material.

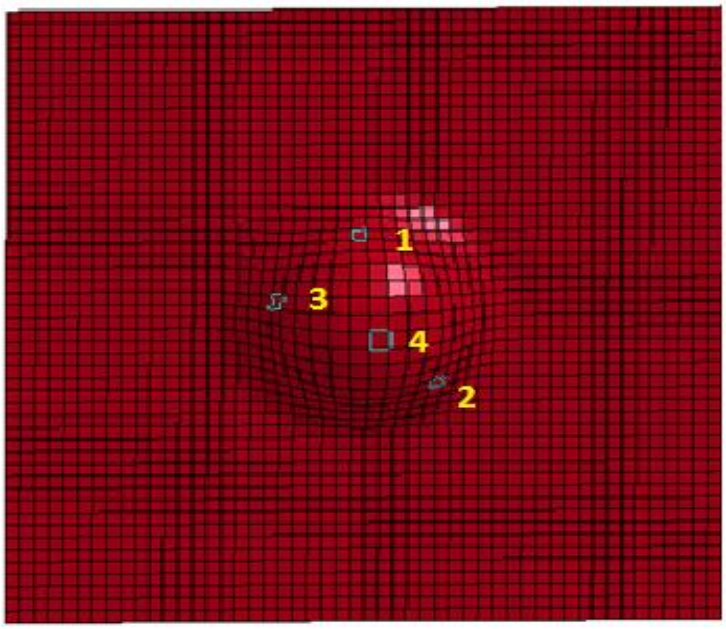
1
3
4
2

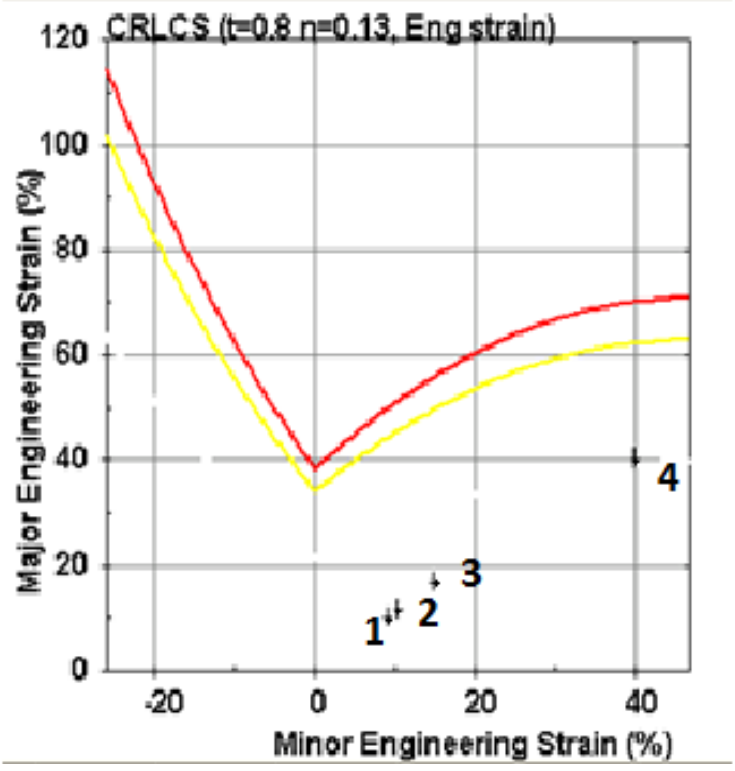
CRLCS (r=0.8 n=0.13, Eng strain)
Major Engineering Strain (%)
Minor Engineering Strain (%)
120
100
80
60
40
20
0
-20
0
20
40
1
2
3
4

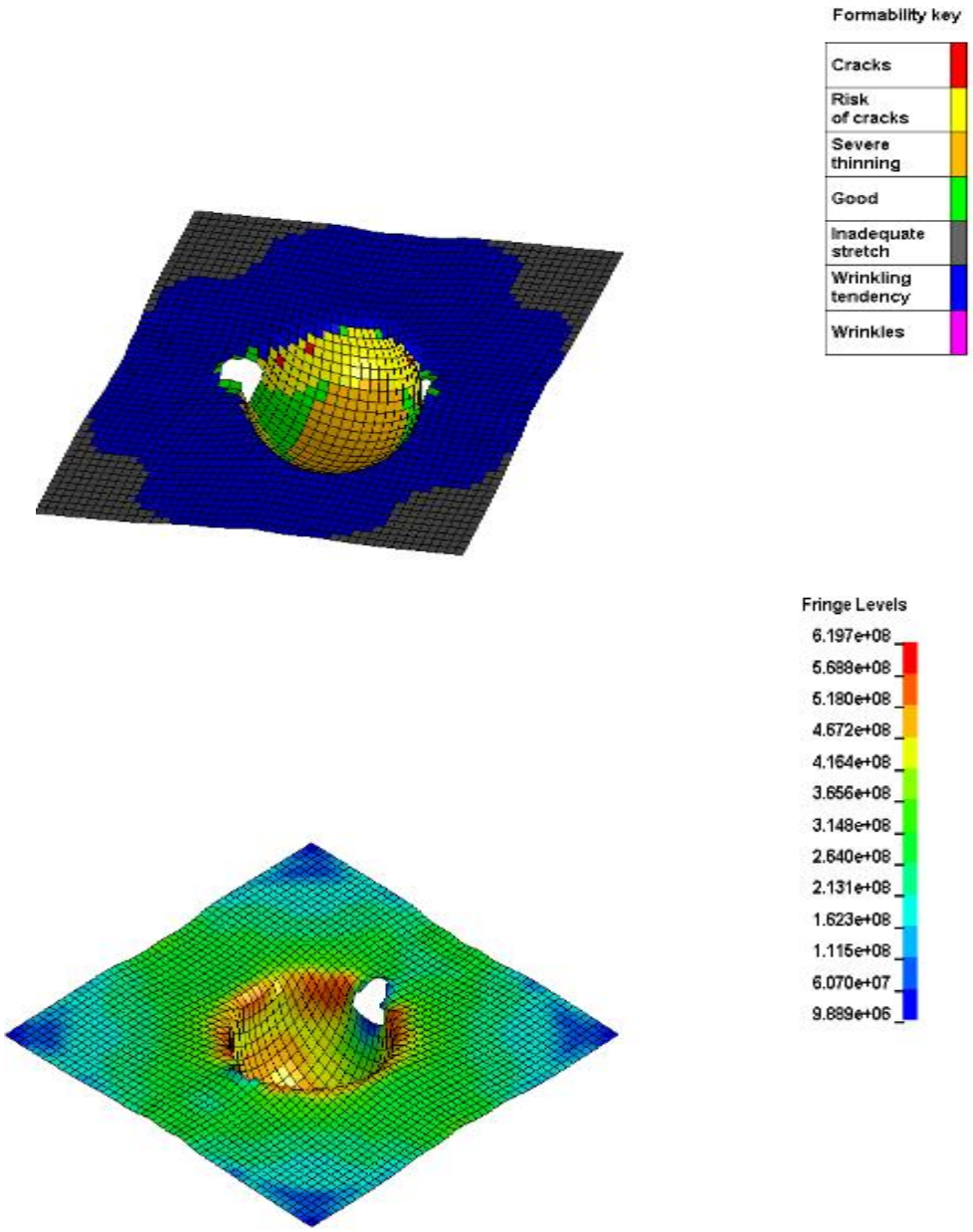

Fig 4.6 FEA results of cupping test with specimen material property plastic kinematic a) FE model of specimen, b) Formability diagram, c) FLD curve and strains at selected points d)Von mesis stress of the specimen

5.3 Material: Linear piecewise plasticity

The Fig 4.7 shows the FEM model for the cupping test. Few points on the part has been selected to get the FLD curves. 1,2,3 and 4 are shown in the FEM model. Fig 4.7(c) shows the formability diagram. Fig 4.7(d) shows the von mesis stress on the material.

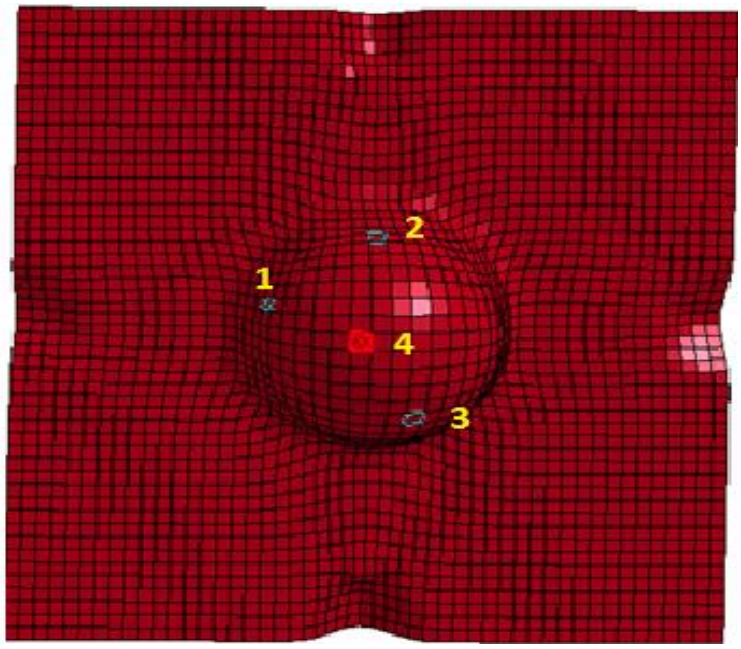
1
2
3
4

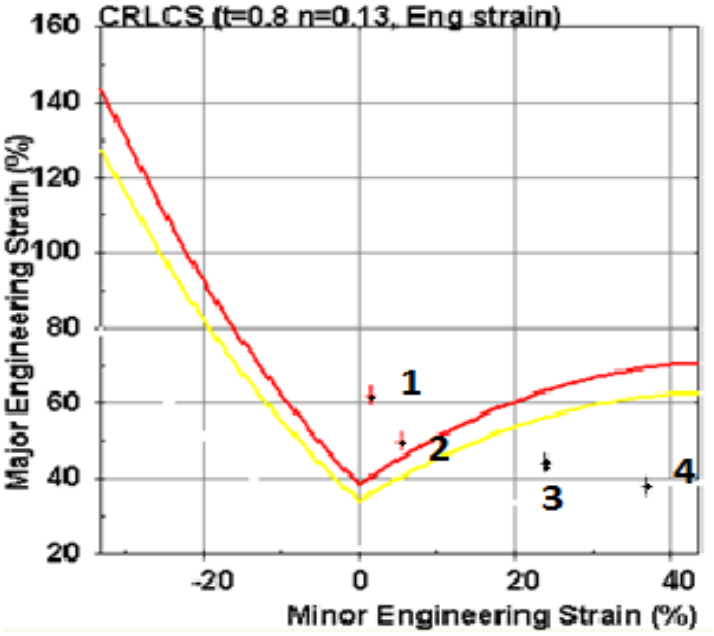
CRLCS (t=0.8 n=0.13, Eng strain)
Major Engineering Strain (%)
Minor Engineering Strain (%)
160
140
120
100
80
60
40
20
-20
0
20
40
1
2
3
4

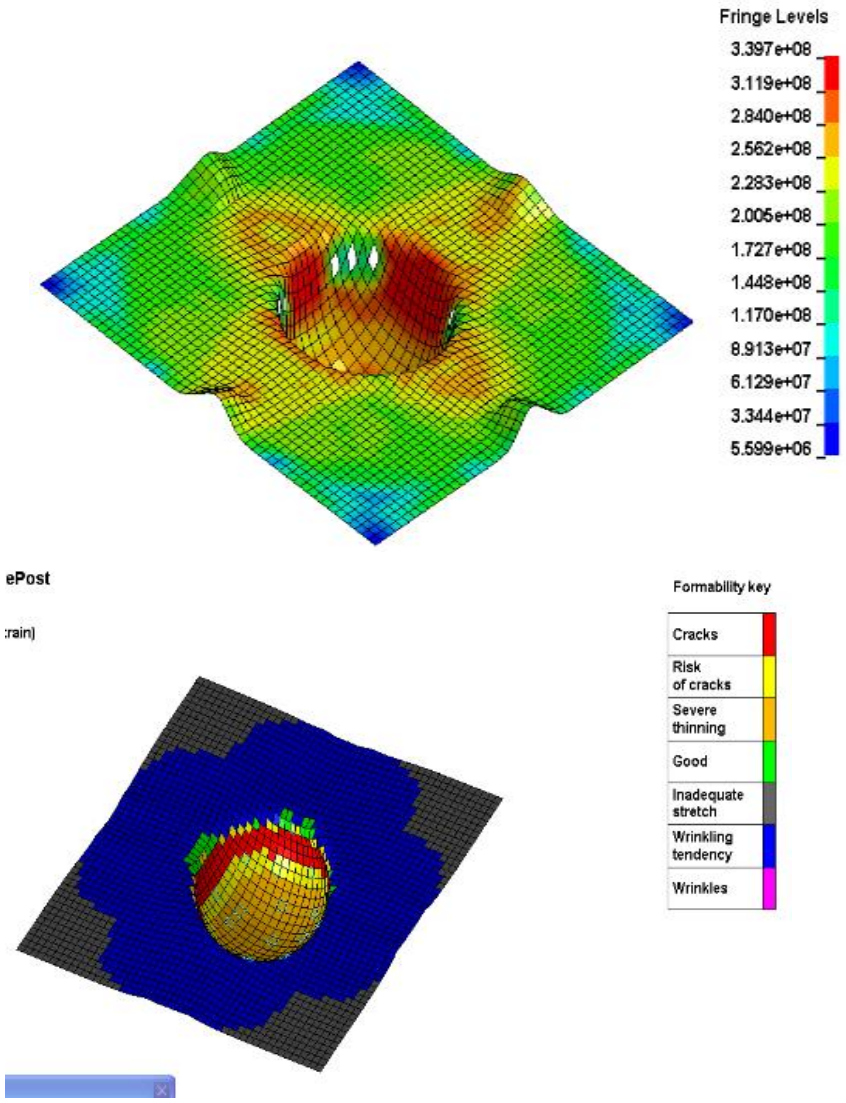

Fig 4.7 FEA results of cupping test with specimen material property plastic kinematic a) FE model of specimen, b) Formability diagram, c) FLD curve and strains at selected points d)Von mesis stress of the specimen

5.4 Reaction force v/s time.

The two graphs shows the reaction force v/s time for the three different material properties linear piecewise plasticity, powerlaw plasticity and plastic kinematic. For these material the graph 4.8 shows with the mesh size 3mm and graph 4.9 shows the mesh size of 0.6mm. For this materials when the thinning co efficient is added, mesh size does not affects the reaction forces as we can see clearly from the two graphs. But if the thinning factor is not added for the materials the reaction force is different as we can see in the graph 4.10. 4.11 represents the graph reaction force v/s time with the mesh size 0.6.

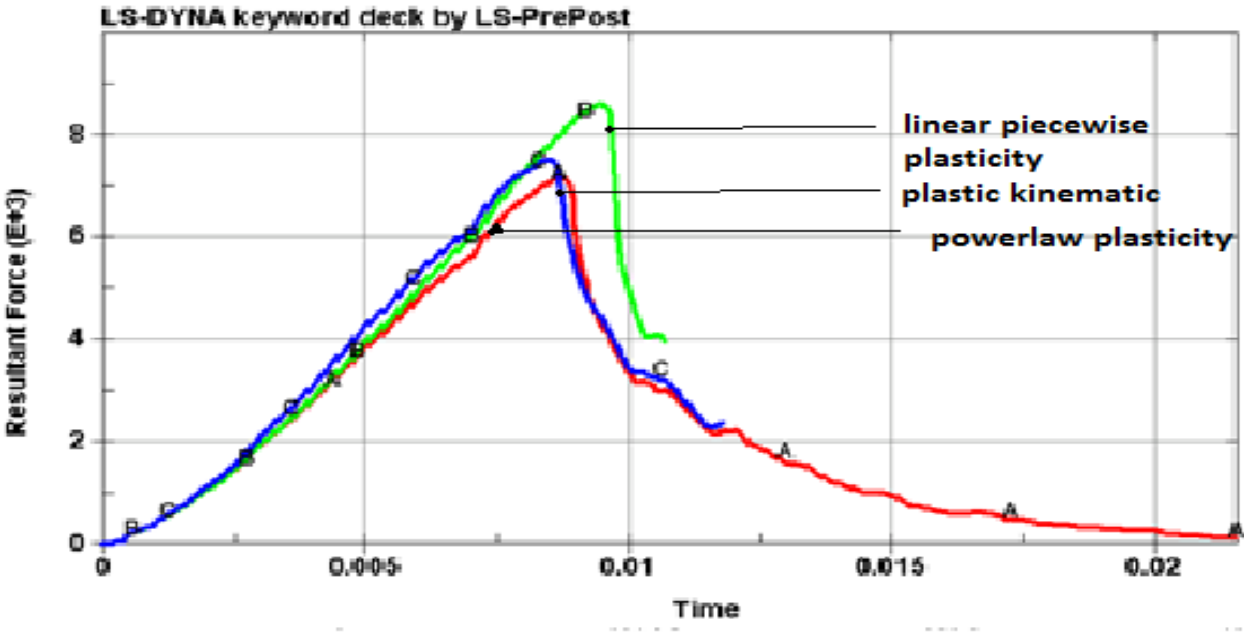

Fig 4.8 reaction force v/s time for the mesh size 3mm with thinning factor

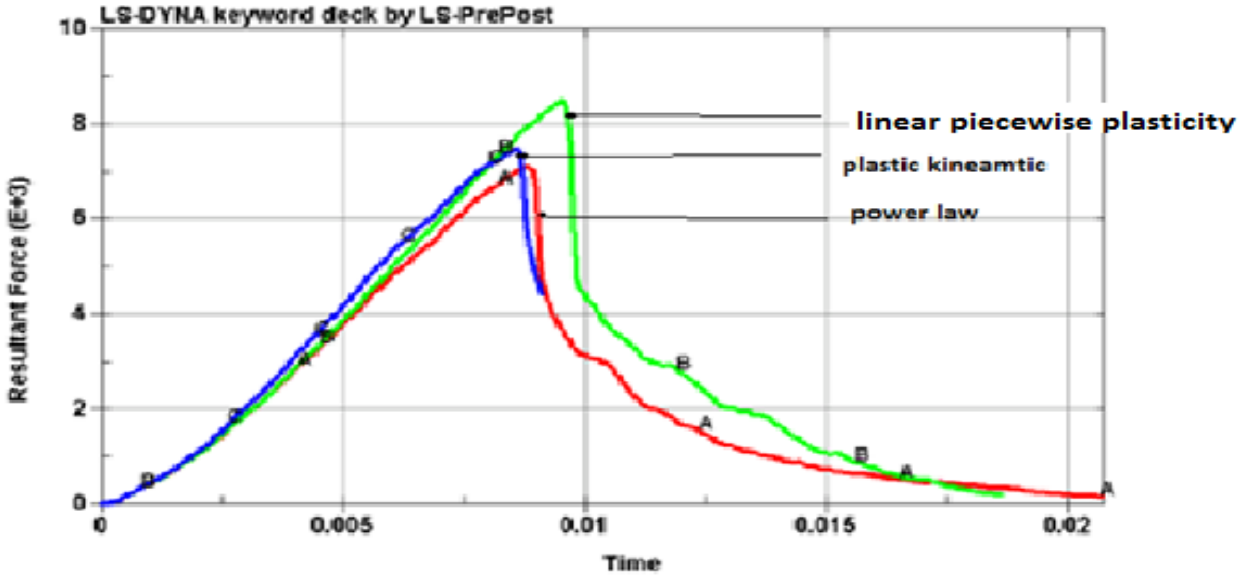

Fig 4.9 reaction force v/s time for the mesh size 0.6mm with thinning factor

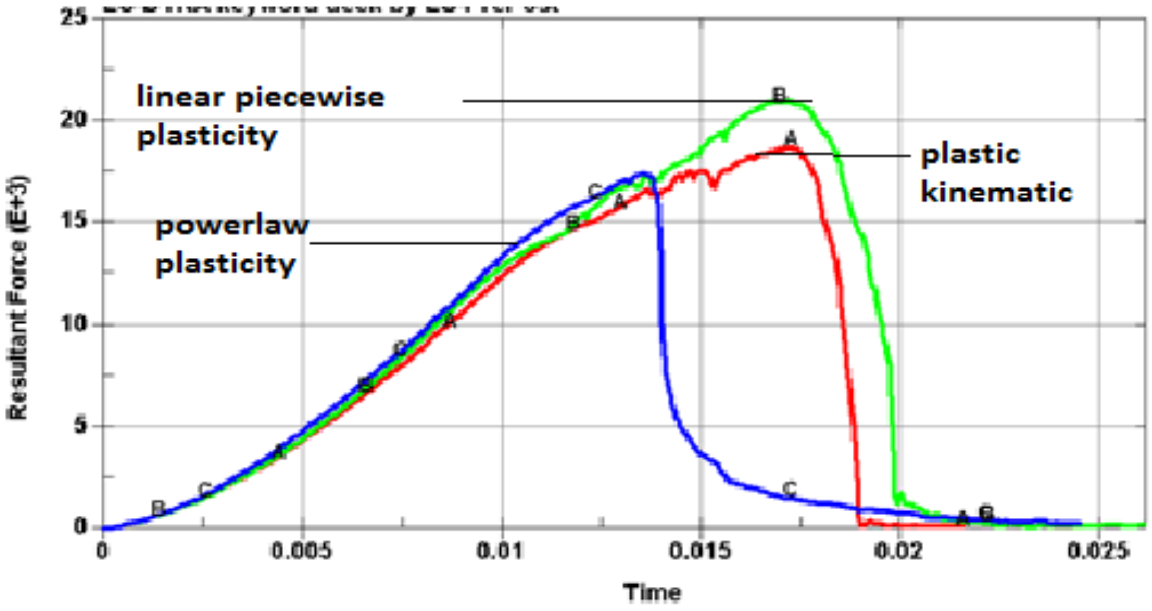

Fig 4.10 reaction force v/s time for the mesh size 3mm

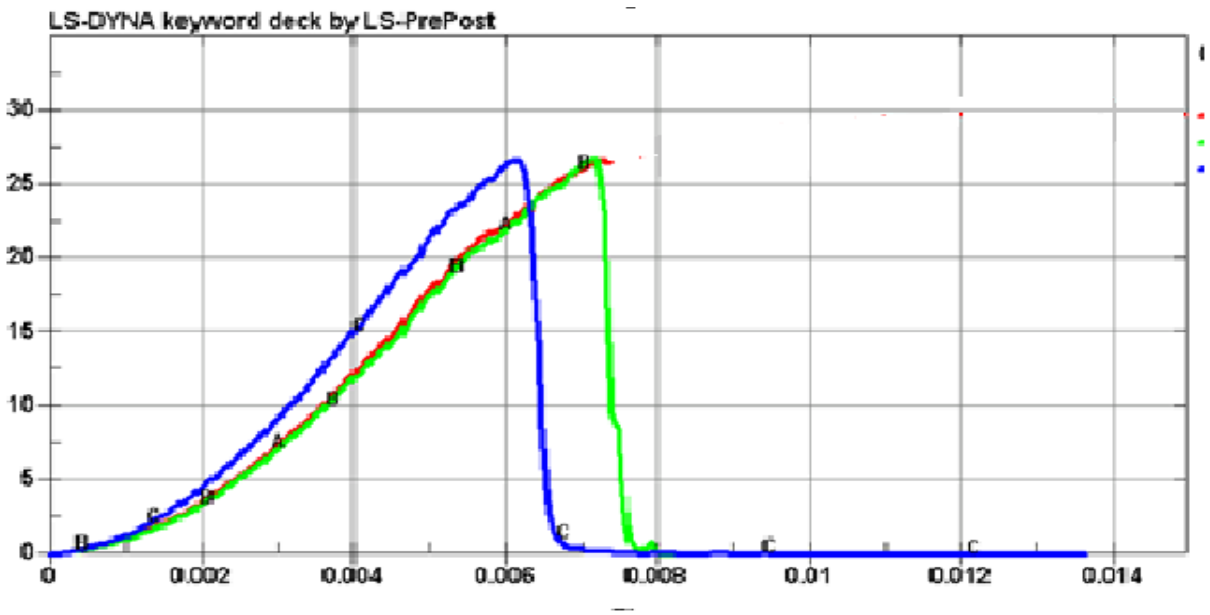

Fig 4.11 reaction force v/s time for the mesh size 0.6mm

5.5 Comparison of experimental results with the different material properties and thinning factors

In the graphs 4.12, 4.13, 4.14 shows the experimental results of FEM results for the material properties linear piecewise plasticity, powerlaw plasticity and plastic kinematic. In this graph there are three curves, blue curve represents the experimental and orange represents the material with the thinning factor(shell 1) and the grey curve represents the thinning factor(shell 4).

Shell 1-membrane straining causes thickness change.

Shell 2- membrane straining causes thickness change, but the elastic strains are neglected for the thickness.

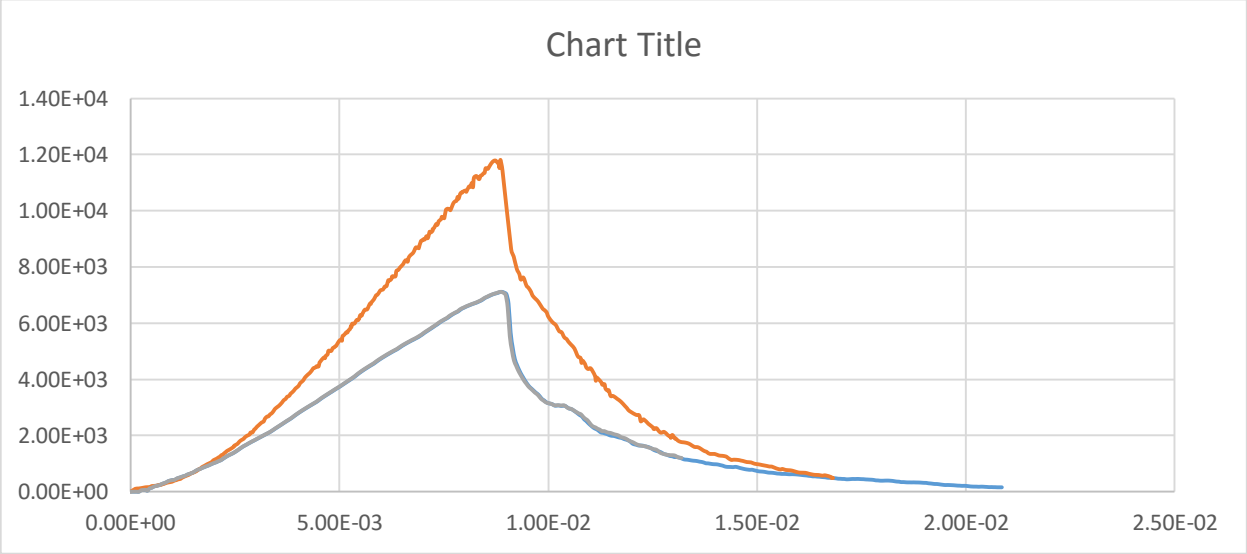

Fig 4.12 comparison of reaction force v/s displace for the experimental results and thinning factors for the material linear piecewise plasticity

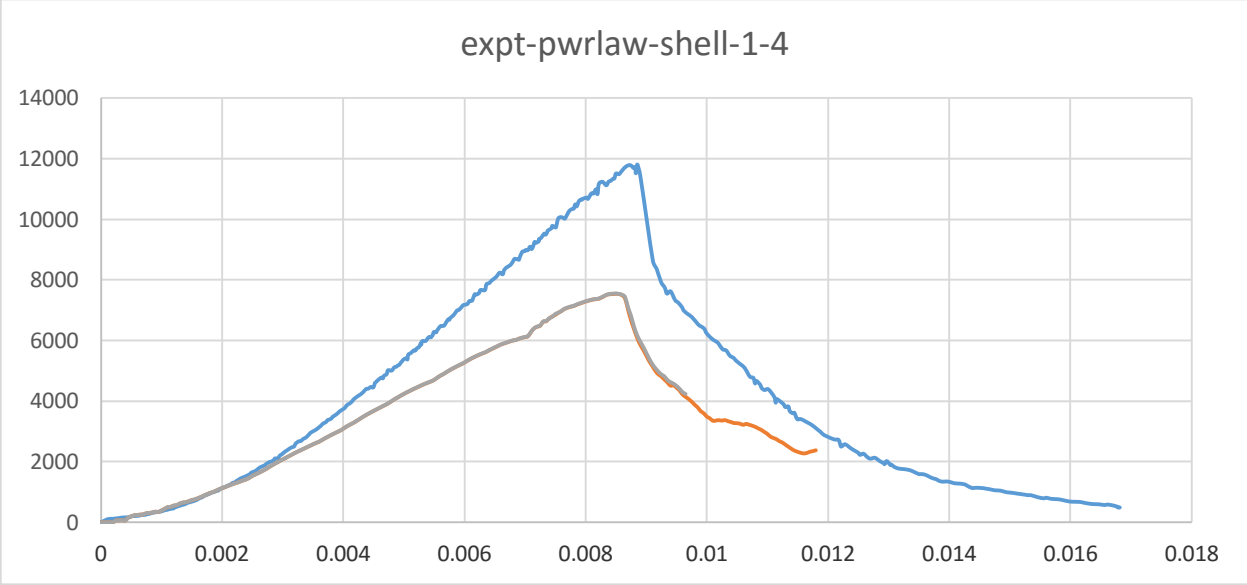

Fig 4.13 comparision of reaction force v/s displace for the experimental results and thinning factors for the material powerlaw plasticity

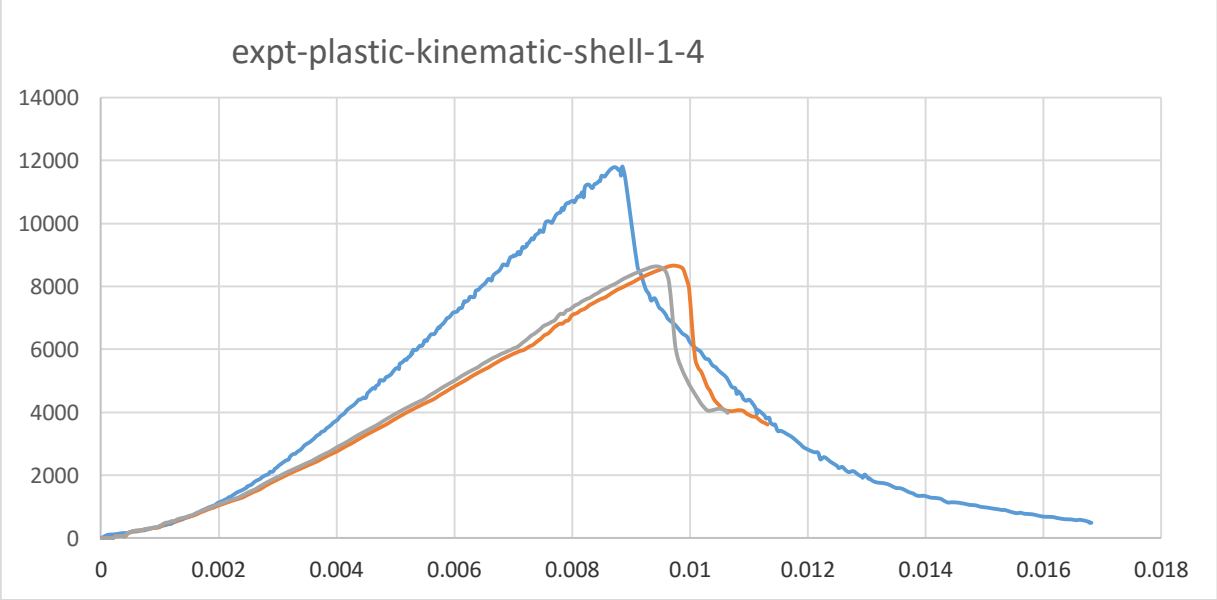

Fig 4.14 comparison of reaction force v/s displace for the experimental results and thinning factors for the material plastic kinematic.

5.6 Comparison of reaction force v/s displacement for the experiment results with the FEM model for the mesh size 0.6mm

The graph 4.15 shows the experimental results with FEM model with the different material properties. In this graph blue curve represents the experimental results. Orange curve shows the plastic kinematic material property. Yellow curve shows the linear piecewise plasticity material property. Grey curve shows the powerlaw plasticity material property.

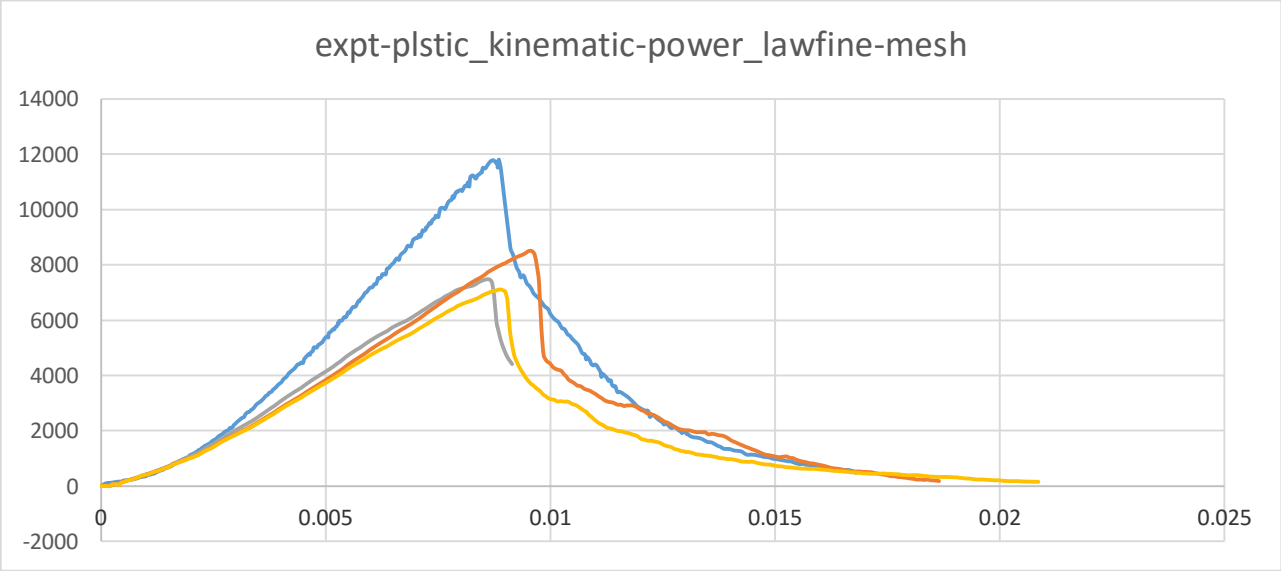

Fig 4.15 comparision of reaction force v/s displace for the experimental results for the mesh size 0.6

Conclusions

1. Comparing the FLD curves obtained from three different approaches (separate points from FE simulation, theoretical curve from LS-Prepost, and theoretical curve from empirical formulas 2.1 and 2.2) we see that separate points from FE results and all curve from LS-Prepost have quite good coincidence. For later analysis the FLD curve can be used for evaluation of metal forming process simulation.

2. Comparing the experimental and simulation results of cupping test we obtain the difference around 30%. Simulation using fine mesh and PowerLaw or Piecewise plasticity material models gives the maximum force of approximately 8.2 kN and in experimental way we are getting approximately 12 kN. Plastic-kinematic material model makes specimens to plastic.

3. Cupping test simulations results also showed the big influence of the thinning option. Allowing the thinning for shell elements we obtain the big influence for the final results. The reaction force decrease about 2÷2.5 times.

4. Comparing the results of cupping test simulations we observe the small influence of FE mesh size to the final results. For fine mesh (element length is about 0.6mm) 10% increase in the reaction force when compared to the initial mesh of 3mm size.

7. References

[1]S. BRUSCHI, T. ALTAN, D. BANABIC, P.F. BARIANI, A. BROSIUS, J. CAO, A. GHIOTTI, M. KHRAISHEH, M. MERKLEIN, A.E. TEKKAYA, *Testing and modelling of material behaviour and formability in sheet metal forming,* CIRP Annals - Manufacturing Technology, Volume 63, Issue 2, 2014, Pages 727-749, ISSN 0007-8506, http://dx.doi.org/10.1016/j.cirp.2014.05.005.

[2] WILHELM RUST, KARL SCHWEIZERHOF, *Finite element limit load analysis of thin-walled structures by ANSYS (implicit), LS-DYNA (explicit) and in combination, Thin-Walled Structures,* Volume 41, Issues 2–3, February 2003, Pages 227-244, ISSN 0263-8231, http://dx.doi.org/10.1016/S0263-8231(02)00089-7.

[3] ERICHSEN, *manual for testing equipment for the quality management*. (http://www.spitec.cl/Spitec/Productos/Erichsen/PDF/1.pdf)

[4] PROF. DR. RIZA GÜRBÜZ Res. Assist. Gül ÇEVİK. *Department of metallurgical and materials engineering*. (http://ocw.metu.edu.tr/file.php/43/Tension_Test_-_ekme_Deneyi.PDF)

[5] MOHAMED HARHASH, OLGA SOKOLOVA, ADELE CARRADÓ, HEINZ PALKOWSKI, *Mechanical properties and forming behaviour of laminated steel/polymer sandwich systems with local inlays – Part 1, Composite Structures,* Volume 118, December 2014, Pages 112-120, ISSN 0263-8223,

[6] MARRAPU BHARGAVA, ASIM TEWARI, SUSHIL K. MISHRA, *Forming limit diagram of Advanced High Strength Steels (AHSS) based on strain-path diagram, Materials & Design*, Volume 85, 15 November 2015, Pages 149-155, ISSN 0264-1275,

[7] C.M.A. SILVA, L.M. ALVES, C.V. NIELSEN, A.G. ATKINS, P.A.F. MARTINS, *Failure by fracture in bulk metal forming, Journal of Materials Processing Technology*, Volume 215, January 2015, Pages 287-298, ISSN 0924-0136, http://dx.doi.org/10.1016/j.jmatprotec.2014.08.023.

[8] BSSA - British Stainless Steel Association. *Material properties*.(http://www.bssa.org.uk/)

[9] ABDULLA MOHAMMAD GOUS SHAIKH & TIPPA BHIMASANKARA RAO. *Sheet Metal Forming Simulations for Heavy Commercial Vehicle Parts by LS-DYNA.* Global Journal of Researches in Automotive Engineering.Volume 13 Issue 1 Version 1.0 Year 2013. Publisher: Global Journals Inc. (USA)

[10] BRADLEY.N.MAKER. *A procedure for spring back analysis using LS DYNA*.Livermore software technology copartation. October

[11] LS DYNA manual. Supports. VOLUME II .Material Models .August 2012.Version 971 R6.1.0. Page nos, 1067.

[12] World Steel Association 2012, *ISBN 978-2-930069-67-8. A white book of steel*. (https://www.worldsteel.org/dms/internetDocumentList/press-release-downloads/2013/The-white-book-of-steel/document/The%20white%20book%20of%20steel.pdf)

[13] SURAJIT K PAUL, G MANIKANDAN AND RAHUL K VERMA. *Prediction of entire forming limit diagram from simple tensile material properties.* 22 November 2012. Page nos, 387

[14] EFUNDA. *Engineering fundamentals*. (http://www.efunda.com/home.cfm)

[15] *Book of mechanical fundamentals*. (http://mechanical 2020.blogfa.com/category/89/%D9%81%D9%88%D8%B1%D8%AC-Forging)

[16] Manual for manufacturers. *San Diego hardware and plumbing.* (http://www.hardwaresource.com/hinge-resource-center/hinge-information/hinge-history/hinge-fabrication-methods/)

[17] DAVIS, JOSEPH R; HANDBOOK COMMITTEE, ASM International (2001-08-01). *Copper and copper alloys".* Page nos,325.

[18] NIKIL.R.DHAR. *Sheet metal-forming-processes. Dept. of industrial engineering.* Published on Jan 14, 2013. Page nos. 34. (http://www.slideshare.net/sahilslideshare/sheet-metalformingprocesses)

[19] YOANN DAHAN, YVAN CHASTEL, PATRICK DUROUX, JO¨EL WILSIUS, PHILIPP HEIN, ELISABETH MASSONI. *Procedure for the Experimental Determination of a Forming Limit Curve for Usibor 1500 P.* 16 Feb 2011. Hungary. 8 p.,

[20]. *I*NG. STANISLAV NÉMETH, ING. ANNA ŠÚŇOVÁ ,PROF. ING. EMIL EVIN, CSC. TECHNICAL UNIVERSITY OF KOŠICE FACULTY OF MECHANICAL ENGINEERING DEPARTMENT OF TECHNOLOGIES AND MATERIALS. *EXPERIMENTAL TECHNIQUES FOR DETERMINATION OF LIMIT DEFORMATIONS OF HIGH-STRENGHT STEEL*. 28/2013

[21] I.A. BURCHITZ. *Improvement of Springback Prediction in Sheet Metal Forming*. Strategic Research programme of the Netherlands Institute for Metals Research. Page nos 15

[22]. C.M.A. SILVA, L.M. ALVES, C.V. NIELSEN, A.G. ATKINS, P.A.F. MARTINS, *Failure by fracture in bulk metal forming*, Journal of Materials Processing Technology, Volume 215, January 2015, Pages 287-298, ISSN 0924-0136, http://dx.doi.org/10.1016/j.jmatprotec.2014.08.023.

[23] U.S. DIXIT, S.N. JOSHI, J.P. DAVIM, *Incorporation of material behavior in modeling of metal forming and machining processes*: A review, Materials & Design, Volume 32, Issue 7, August 2011, Pages 3655-3670, ISSN 0261-3069, http://dx.doi.org/10.1016/j.matdes.2011.03.049.